ARTICLE INFO:
Received : November 16, 2016
Revised : March 14, 2018
Accepted : March 23, 2018
CT&F - Ciencia, Tecnologia y Futuro Vol 8, Num 1 June 2018. pages 5 - 29
DOI : https://doi.org/10.29047/01225383.88

ecopetrol
ctyf@ecopetrol.com.co

PROVENANCE AND DIAGENESIS FROM TWO STRATIGRAPHIC SECTIONS OF THE LOWER CRETACEOUS CABALLOS FORMATION IN THE UPPER MAGDALENA VALLEY: GEOLOGICAL AND RESERVOIR QUALITY IMPLICATIONS

PROCEDENCIA Y DIAGÉNESIS DE DOS SECCIONES ESTRATIGRÁFICAS DE LA FORMACIÓN CABALLOS EN EL VALLE SUPERIOR DEL MAGDALENA: IMPLICACIONES EN LA GEOLOGÍA Y LA CALIDAD DEL RESERVORIO

Duarte, E.[a]; Cardona, A.[a]; Lopera, S.[a]; Valencia, V.[b]; Estupiñan, H.[c]*

ABSTRACT

The Aptian-Albian Caballos Formation is a proven reservoir in the oil producing basins of the Upper Magdalena Valley and Putumayo (Colombia), characterized by wide variation in its petrophysical properties. Integrated provenance, diagenetic and basic petrophysical analyses are presented from two stratigraphic sections of the Caballos Formation in the Upper Magdalena Valley (Ocal and Cobre creeks) in order to test regional geological models, and to relate compositional and diagenetic factors with the reservoir quality.

Sandstones from the Caballos Formation document a change from texturally immature- subarkoses, litharenites to quartz arenites. High quartz contents, the presence of feldspar, sedimentary, metamorphic and volcanic lithic suggest mixed provenance, with a major contribution from sedimentary sources. U-Pb dating of detrital zircons reveals age populations that include contributions from Precambrian, Permian, Triassic and Jurassic rocks. These data, together with the compositional trends, suggest that source areas likely include adjacent massifs from the eastern segment of the Upper Magdalena Valley with similar compositional and temporal characteristics (Garzón and Macarena Massifs for the southeastern Ocal Section, and the Upper Magdalena Valley massifs and the eastern flank of the Central Cordillera; Ocal Section). The changes in compositional features and detrital geochronology between the upper and lower members of both sections suggest a change in source areas, associated with the erosion and depletion of adjacent uplifts, and the increasing dominance of more distal eastern and western sources, which reflect the end of tectonic instability and the deepening of the basin.

The presence of quartz, feldspar, and lithic rock fragments have a major impact on the porosity and permeability of Caballos Formation sandstones. Porosity values are lower in the lower member of the Caballos Formation where diagenesis has altered abundant feldspar and lithic rock fragments to authigenic pore-filling clays. Higher porosity and permeability values found in the upper member of the Caballos correspond to a combination of higher quartz contents and the dissolution of meta-stable components during late diagenesis

KEYWORDS / PALABRAS CLAVE

Caballos Formation | Cretaceous | Provenance | Quality of reservoir rock Diagenesis | Detrital Zircon.
Formación Caballos | Cretácico | Procedencia | Calidad del reservorio, Diagenesis | Circón Detrítico.

AFFILIATION

[a]Departamento de Procesos y Energía, Universidad Nacional de Colombia, Sede Medellín, Carrera 80 No 65-223 - Campus Robledo, Medellín, Colombia.
[b]School of the Environment, 642812, Washington State University, Pullman, USA
[c]Departamento de Materiales y Minerales, Universidad Nacional de Colombia, sede Medellín, Colombia.
*email: ejduarteg@unal.edu.co

RESUMEN

La Formación Caballos hace parte de la cuenca del Cretácico Inferior que caracteriza el Oriente Colombiano, y es un almacenador probado en las cuencas productoras del Valle Superior del Magdalena y el Putumayo (Colombia), que se caracteriza por una amplia variación en sus propiedades petrofísicas. En el presente articulo se presentan análisis de petrografía, minerales pesados, geocronología en circones detríticos, SEM y DRX, integrados con análisis petrofísicos básicos de porosidad y permeabilidad en los miembros inferior y superior de dos secciones de la Formación Caballos en el Valle Superior del Magdalena (Quebrada el Ocal y el Cobre), con el fin de reconstruir su procedencia y diagénesis aportando a la comprensión de la historia de la cuenca y evaluando los factores composicionales y diagenéticos que afectan la calidad del reservorio.

Las areniscas de la Formación Caballos varían entre subarcosas, litoarenitas y cuarzoarenitas. Los altos contenidos de cuarzo, la presencia de feldespato, líticos sedimentarios, líticos metamórficos y volcánicos sugieren una fuente mixta. Las poblaciones de circones detríticos con edades Precámbricas, Pérmicas y Triásicas y las características composicionales de las areniscas sugieren que las áreas fuentes podrían incluir macizos adyacentes con características composicionales y temporales semejantes a los actuales incluidos en Valle Superior, Macizo de Garzón y Macarena (Sección El Ocal), y el Valle Superior del Magdalena y la Cordillera Central (Sección El Cobre). Los cambios en las características composicionales y la geocronología en circones detríticos entre los miembros superior e inferior de ambas secciones, sugieren un cambio en áreas fuentes, asociado al agotamiento de los altos de basamento adyacentes, a cambios a lo largo de la componente de rumbo en el estilo estructural entre zonas adyacentes y la aparición de fuentes cada vez más orientales y occidentales, que reflejan el fin de la inestabilidad tectónica y la profundización de la cuenca.

Al comparar los análisis de porosidad y permeabilidad con las características texturales, composicionales y la historia diagenética en las dos secciones estudiadas, se sugiere que la presencia de cuarzo, feldespato y líticos son un factor condicionante de la porosidad. En el miembro inferior donde son más abundantes estos dos últimos, los valores de porosidad son menores, ya que fueron transformados en arcilla y generan altos contenidos de pseudo-matriz. Ya para el miembro superior de la Formación Caballos la alta porosidad y los mejores valores de permeabilidad estarían relacionada con mayores contenidos de cuarzo y una mayor disolución de partículas del armazón durante las fases diagenéticas tardías.

Estos resultados en conjunto con los trabajos anteriores; indican que la heterogeneidad en las propiedades petrofísicas de la Formación Caballos, además de ser consecuencia de las características ambientales, está controlada por la composición y la historia diagenética.

1. INTRODUCTION

The Lower Cretaceous Caballos Formation exposed in the Upper Magdalena Valley, has been related either to the Cretaceous extensional basins that characterizes the eastern sector of the Colombian and Ecuadorian Andes [1], or to a foreland basin associated to compressive event of this age that which has been mostly recognized in the Cordillera Real of Ecuador [2,3].

Seismic interpretation, stratigraphic and petrographic observations [4,5], suggest that the accumulation of the Caballos Formation in the Upper Magdalena Valley was limited to the east and west by structural highs that may correlate with the Garzón paleo massif and proto-Central Cordillera.

Given the oil-producing nature of this formation in the Upper Magdalena Valley and Putumayo basins, several studies that have deal with its reservoir qualities have suggested the existence of lateral environmental variations, which are expressed by the strong lateral variations on facies type and thickness [5], or to the presence of calcareous allochemicals and the variation in the heat flow near the Lower Cretaceous fault areas, which would control the dissolution and the generation of secondary porosity [6].

This paper presents petrographic, heavy mineral analysis, detrital zircon U-Pb Geochronology, and basic petrophysical analysis from two stratigraphic sections of the Caballos Formation exposed in the Neiva and Girardot subbasins within the Upper Magdalena Valley **Figure 1**.

The new results make it possible to characterize the provenance of the Caballos Formation and to review the source are configuration during basin filling in the Aptian- Albian. Additionally, the analysis of the relationship between petrophysical attributes and petrographic characteristics suggests that the quartz and feldspar contents, the formation of pseudo-matrix and dissolution processes affect the quality of the siliciclastic facies in the Caballos Formation.

2. THEORETICAL FRAME

GEOLOGICAL FRAMEWORK

The geological record between the Jurassic and the Early Cretaceous in the Central and Eastern Colombian Andes is related to the subduction of the Farallón plate, and several extensional events associated with the fragmentation of Pangea and the formation of the Gulf of Mexico [1], [7]-[10]. This complex tectonic configuration is recorded by the growth of different magmatic arcs during a large part of the Jurassic, and the generation of a series of extensional basins within the continent [11]. During the Lower Cretaceous, the continued formation of the proto-Caribbean and the opening of the Atlantic [12], as well as several collisional events have shape the margin [2].

The Central Cordillera of the Colombian Andes exhibits a Devonian, Permo-Triassic and Jurassic plutonic and metamorphic substrate [2],[13]-[16]. Different Lower Cretaceous clastic sequences are

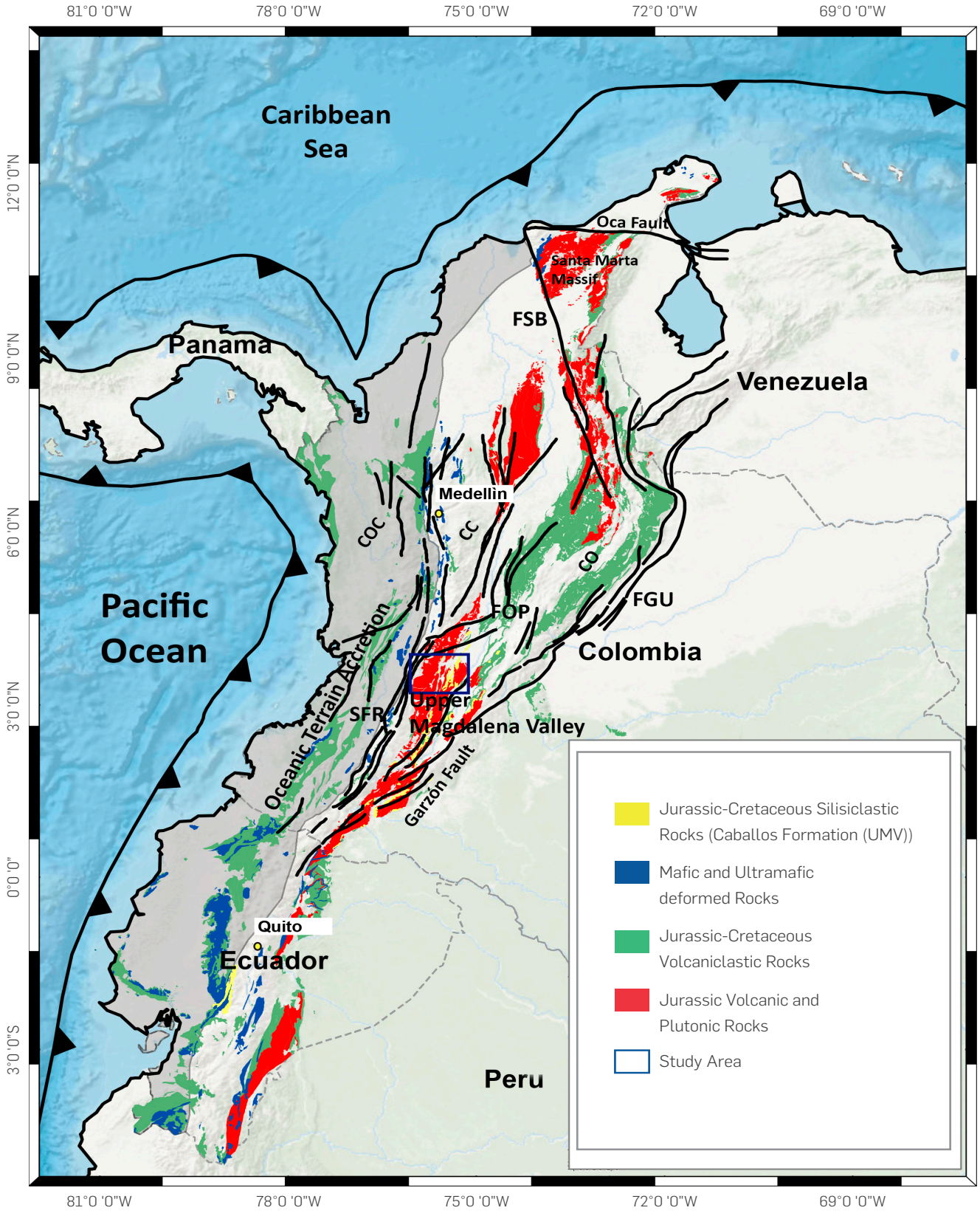

Figure 1. General location of the study area, enclosed in blue box. FSB = Santamarta-Bucaramanga Fault, FGU = Guacaramo Fault, FOP = Otú-Perico Fault, SFR = Romeral Fault System, CO = Eastern Cordillera, CC = Central Cordillera, COC = Western Cordillera. Prepared by us with information compiled [74].

discontinuously deposited over this basement rocks, and are characterized by a transgressive record that extends from the Berrasian to the Albian-Aptian, and ends with the development of oceanic crust and the subsequent construction of a magmatic arc that likely extends to the Upper Cretaceous [10],[17]-[18].

The Eastern Cordillera including its continuation to the south in the Garzón Massif includes a Proterozoic metamorphic rocks with radiometric ages between 980 Ma-1180 Ma [19, 20] and Early to Middle Jurassic granitoids [21], as well as (meta) sedimentary rocks from the Lower to Upper Paleozoic [22]-[24]. An extensive Jurassic to Cretaceous clastic and chemical record with minor Cretaceous gabbroic intrusions overly this Precambrian to Paleozoic rocks [25,26]. The Lower Cretaceous record is characterized by a transgressive nature, associated with conditions of high subsidence within an extensional basin.

In the Middle Magdalena Valley, the clastic record has been similarly associated with an extensional history since the Berrasian-Hauterivian [27,28], which was likely deposited over the volcano-sedimentary and plutonic sequences of Triassic to Jurassic in age. This record is probably characterized by the development of high-energy fluvial environments, followed by a deepening of the basin towards transitional environments in the Aptian [1],[29]-[31]. In the Upper Magdalena Valley, the Putumayo basin and the eastern Ecuadorian basin, sedimentary accumulation began in the Barremian and extends to the Albian-Aptian, and is also characterized by extensive subsidence and a transgressive nature, deposited in a continental to transitional environments [32,1], which has been interpreted as associated with an extensional [1] or collisional record [2,3].

Later, the stratigraphic record present in the Eastern Cordillera and the Middle and Upper Magdalena Valley is characterized by stable tectonic conditions, at least between the Turonian and the Campanian [33] **Figure 2**.

LOWER CRETACEOUS RECORD IN THE UPPER MAGDALENA VALLEY

The Upper Magdalena Valley is a depression bound by the Central and Eastern Cordillera characterized by 400 km in length, and a width that can reach 65 km.

Based on the lateral variations of facies, it has been suggested that the basin where the Caballos Formation was accumulated was characterized by a block related paleotopography [34,5], bounded by identifiable structural highs in the seismic lines, which include an extensive paleo-high to the east identified as Arco del Vaupés, that may include segments of the Garzón Massif and Serranía de la Macarena, and to the west another topographic high that could be related to the proto-Central Cordillera.

The Mesozoic sedimentary fill of the Upper Magdalena Valley comprises units that span from the Triassic to the Cretaceous (**Figure 2**). The Triassic-Jurassic includes continental clastic sediments, a calcareous record, effusive and pyroclastic volcanism, as well as plutonic rocks of acid to intermediate composition, which have been grouped in the Luisa, Payandé and Saldaña formations respectively [25]. Different intermediate to felsic plutonic bodies with an extensive geological history between 190 Ma and 139 Ma intrude some of these sedimentary units and the older metamorphic basement [35].

In the Lower Cretaceous, sedimentation possibly begins during the Barremian with the deposition of the Yaví Formation [5], which is characterized by continental siliciclastic facies and pyroclastic volcanic material. These rocks are in angular unconformity on the pre-Cretaceous basement and in gradational contact with the overlying Albian-Aptian Caballos Formation [36].

The Caballos Formation is characterized by mix clastic and calcareous sedimentation accumulated in transitional and continental environments, and reach a maximum thickness of 450m [32, 37], which can be divided into three members [38]-[41].

The lower member is characterized by intercalations of mudstones and sandstones of up to 250m of thickness [37]. Towards the base it exhibits thin beds of coarse-grained to massive conglomeratic sandstones, with low-angle lamination or trough cross stratification [42,6]. This member of Aptian in age [43], has been related to fluvial and estuarine environments [40,41,6].

The middle member includes muddy and calcareous intercalations with thin packets of sandstones. This succession has a thicknesses between 80m and 100m [44,32,42,6], and has been related to coastal environments [41,34], having been accumulated during the Upper Aptian [43].

The upper member of the Caballos Formation exhibits layers of medium to fine grain sandstones with interspersed mudstones, whose maximum thickness can reach 60m [45]. It has been related to fluvio-deltaic environments and coastal areas, which likely accumulated during the Middle Albian [43].

Conformable with the Caballos Formation are intercalations of shales, black chert, and micritic and esparitic limestones from the Villeta Group, that were accumulated in a shallow platform environment during the Campanian and Cenomanian [43].

3. EXPERIMENTAL DEVELOPMENT

PETROGRAPHY AND IMAGE ANALYSIS

Twenty-one sandstone samples from the Caballos Formation collected in the Ocal Creek section (Huila) and in the Cobre Creek (Tolima) in the Upper Magdalena Valley were petrographically analyzed.

Roundness and sphericity was determined in 100 grains [46], and 300 grains were counted in accordance with the Gazzi-Dickinson and Indiana methods [47]. Petrographic discrimination of quartz types was carried out on 100 grains [48].

The porous space was measured in 14 samples by analyzing the images obtained in an Epson V500 scanner, with two different software packages: IMAGEJ-JPOR® [49] and JMICROVISION® [50].

HEAVY MINERALS

Heavy minerals were analyzed in nine sandstone samples from the lower and upper members of the Caballos Formation.

The sandstones were disintegrated using a metallic mortar and sieved using 400µm disposable mesh. Subsequently, sodium

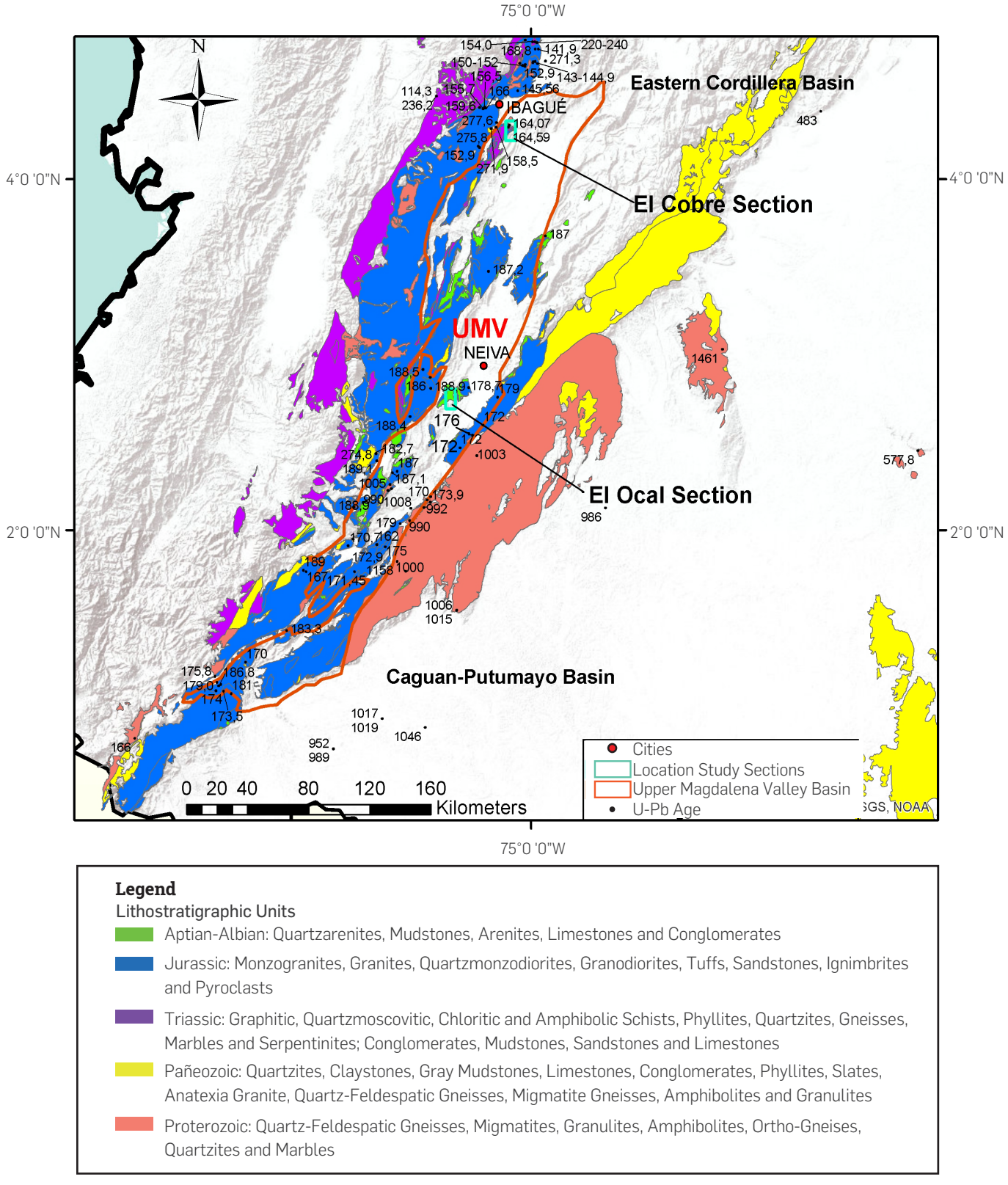

Legend

Lithostratigraphic Units

- Aptian-Albian: Quartzarenites, Mudstones, Arenites, Limestones and Conglomerates
- Jurassic: Monzogranites, Granites, Quartzmonzodiorites, Granodiorites, Tuffs, Sandstones, Ignimbrites and Pyroclasts
- Triassic: Graphitic, Quartzmoscovitic, Chloritic and Amphibolic Schists, Phyllites, Quartzites, Gneisses, Marbles and Serpentinites; Conglomerates, Mudstones, Sandstones and Limestones
- Pañeozoic: Quartzites, Claystones, Gray Mudstones, Limestones, Conglomerates, Phyllites, Slates, Anatexia Granite, Quartz-Feldespatic Gneisses, Migmatite Gneisses, Amphibolites and Granulites
- Proterozoic: Quartz-Feldespatic Gneisses, Migmatites, Granulites, Amphibolites, Ortho-Gneises, Quartzites and Marbles

Figure 2. Geological map for the block studied in the Upper Magdalena Valley Basin. Source: Modified from [74]. The study areas in the Caballos Formation are indicated by a green box.

polyungstane was used to separate the fraction with a density > 2.89 g / cm^3. The grains were immersed in Meltmount® with a refractive index of 1.539. Up to 300 translucent grains were counted using the line method [51].

DETRITAL ZIRCON U-PB GEOCHRONOLOGY

U-Pb detrital zircons from four-samples were analyzed with the U-Pb LA-ICP-MS (Laser Ablation Inductively Coupled Plasma Mass Spectrometry) technique. Preparation was carried out in the Zirchron LLC laboratories and the analyses were conducted at the Washington State University in Pullman, United States [52]. The Plešovice standard with an age of 337.1 ± 0.4 Ma was used for this study [53]. Analytical results are present in **Appendix 1.**

The analyses were performed on the zircon cores in order to avoid zircons with complex histories [54]. Individual ages for each sample were processed and plotted using Probability Density Plots (PDP) with the Isoplot 3.62® program [55]. Individual analyses that exceeded 10% analytical error and 20% unconformity were discarded for interpretations and discussion. However, unconformity was not evaluated for grains less than 500 Ma, given that the abundance of ^{207}Pb cannot be measured with sufficient precision to evaluate the unconformity between the ages ^{206}Pb/^{238}U and ^{206}Pb/^{207}Pb [56]. In addition, **Appendix 2** shows the Tera- Wasserburg concordia diagrams prepared for each of the analyzed samples.

PETROPHYSICAL ANALYSIS

Porosity was calculated by means of Boyle porosimetry in 10 rock core samples, and through the gravimetric method in an irregularly shaped samples [57]. Samples were taken in outcrops from both study sections (**Figures 3 and 4**) with a portable drill. Permeability tests were performed on 7 samples following the procedure provided by [58], using a confining pressure of 2000 psi similar to those found in the fields relating to the Caballos Formation in the Magdalena Valley.

SCANNING ELECTRON MICROSCOPY (SEM) AND X-RAY DIFFRACTION.

In order to analyze the clayey fraction, a total of four samples were analyzed in the JEOL JSM-5910LV Scanning Electron Microscope, with a BSE detector and an EDX spectrometer at Universidad Nacional de Colombia (Medellín). The clayey fraction less than <2µm was analyzed after removing organic matter and carbonates with Morgan's solution and 35% hydrogen peroxide. The standard conditions were Kα1 = 1.540598, 45 kV; 40 mA with a 2 theta between 3° and 72° (with a step of 300 seconds in total and an angle of 0.0334°). The semi-quantitative estimate followed the protocol provided by [59].

4. RESULTS

Seven samples from the lower and upper members of the Caballos Formation were sampled in the Ocal section [41] (**Figure 3**). Whereas for the Cobre section [60] we have select nine samples also from the Lower and Upper members (**Figure 4**).

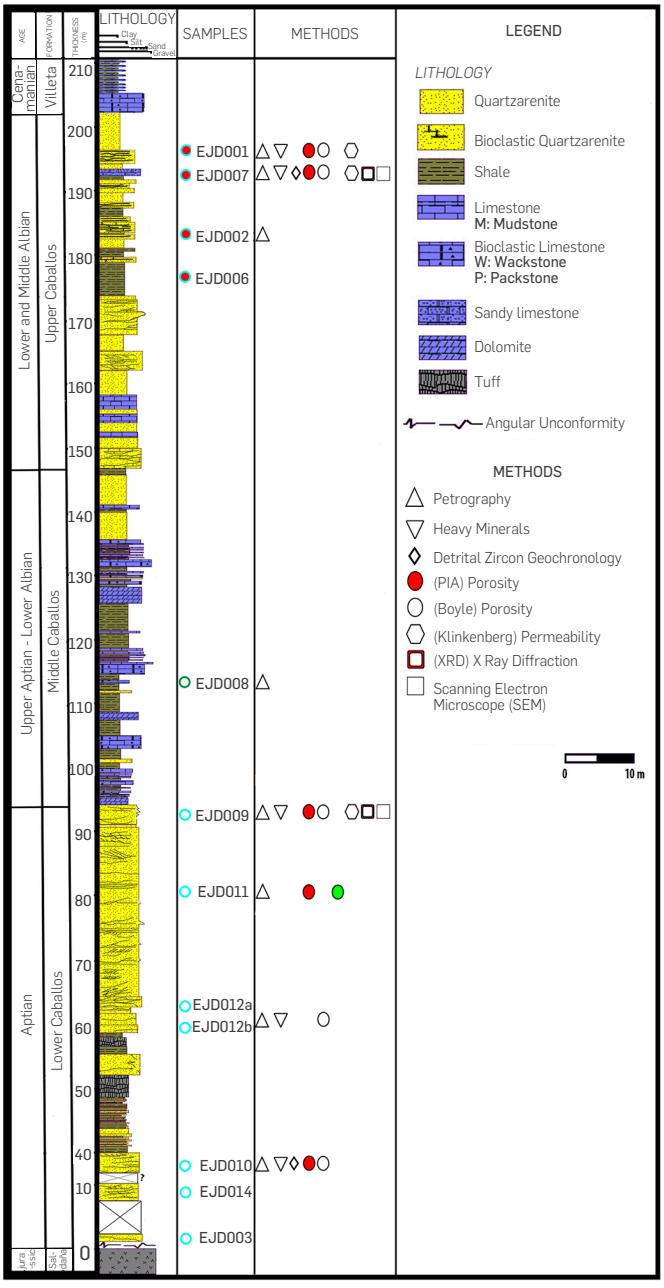

Figure 3. Lithostratigraphic column of the study area in the southern part of the Upper Magdalena Valley basin in Ocal Creek. Modified from [36].

PETROGRAPHY

EL OCAL CREEK SECTION:
Sandstones from the lower member are of medium to fine grain, subangular and sub-rounded, with both low and high sphericity and poor to moderate selection. The contacts between the grains are mainly concave-convex and sutured. The matrix content varies between 4% and 18%, and include pseudomatrix associated with the disintegration of mudstone lithics. XRD analysis suggest that the matrix is dominated by the presence of kaolinite and interstratified illite-smectite (**Figure 5, Table 1**).

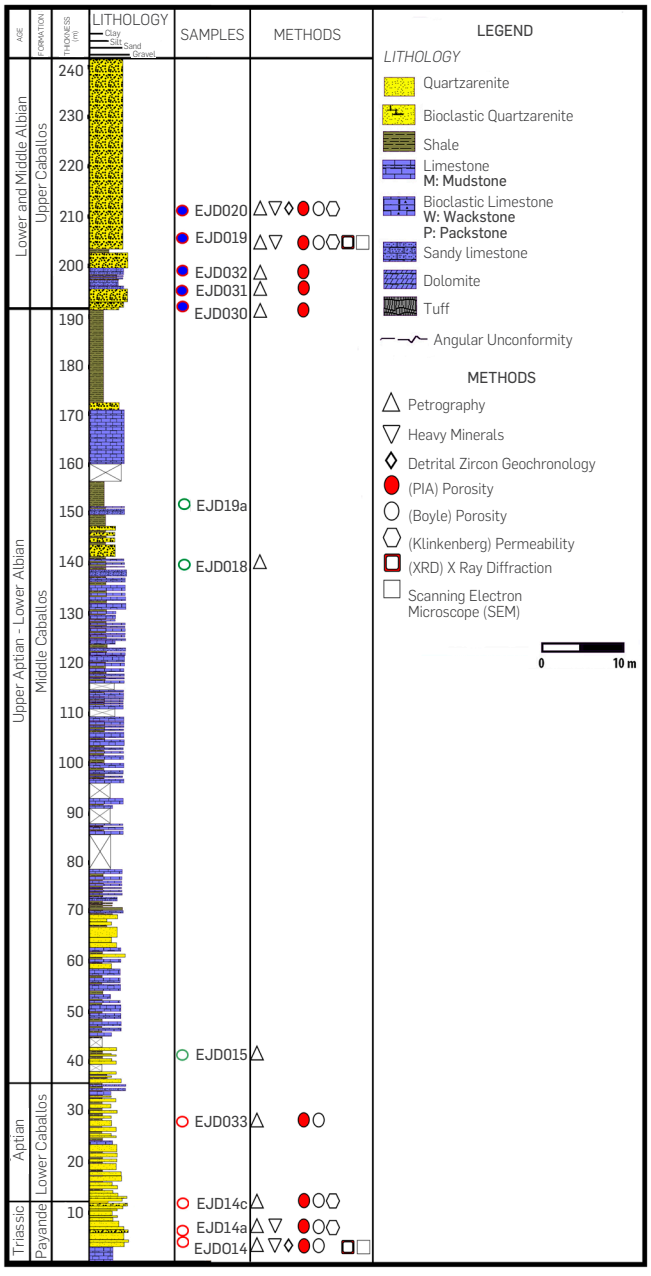

Figure 4. Diagram that represents the Lithostratigraphy of the study area in the northern part of the Upper Magdalena Valley basin in Cobre Creek. Modified from [60,75].

The sandstones are quartz arenites, subarkoses and sublitharenites ([61]; see **Table 1**, **Figure 6**. Quartz grain include monocrystalline quartz with straight extinction and sedimentary and diffuse polycrystalline quartz with more than three grains. Feldspar is less than <7%, and include mainly K-feldspar with a pertitic texture and alteration to clays. Lithics include felsic volcanic and plutonic fragments with quartz and feldspar (**Figure 6**), reddish brown to yellow mudstones and chert, and muscovite schists. Flexed muscovite was also seen in proportions lower than 5%, whereas zircon, epidote, tourmaline, hornblende, calcite and cordierite are present in proportion less than 1%. Siliceous, ferruginous and calcareous cements were identified (3% -14%). It was also common to find organic matter and oil partially covering pores and generally accompanied by epidote, tourmaline and pyrite.

Sandstones of the upper member are of medium size, subangular to sub-rounded, with low to high sphericity and poor to moderate selection. Contacts between grains are mainly tangential, with minor concave-convex and suture. Matrix is mainly fine silt and mud and is present with proportions between 11% and 12% (**Figure 5**). XRD analyses indicate that the most abundant clay minerals are interstratified illite-smectite and kaolinite.

The sandstones are calcareous quartz arenites [61]. Monocrystalline quartz with straight extinction predominates, while sedimentary and diffuse polycrystalline quartz are also present in smaller quantities. Polycrystalline quartz grains are found with 2 and three grain and polygonal to diffuse contacts. Feldspar is less than 7%, and include K-feldspar (microcline) with perthitic texture, whereas the plagioclase is altered to clay minerals. Lithics include mudstone, chert and quatz-feldspar sandstones that are affected by ductile deformation (**Figure 6**). Glauconite is presented in a proportion between 5% and 15%, whereas zircon, epidote, tourmaline, garnet, monazite and diopside are present in proportions below 2%. Calcareous and ferruginous cements were identified (7% -11%).

EL COBRE CREEK SECTION:

Sandstones from the lower member are fine to coarse grain, rounded to sub-rounded grains, low to high sphericity and poor selection. Contacts are tangential, with minor concave-convex and sutured relations. Matrix contents varies between 9% to 18%, and is dominated by clay minerals (6%) (**Figure 5**), that based on the XRD analysis they are mainly illite-smectite and kaolinite (**Table 1**).

Compositionally, the sandstones show appreciable amounts of lithics, and are classified as litharenites, sublitharenites and subarkoses ([61], see **Table 1, Figure 6**). Monocrystalline quartz with a straight and undulatory extinction is the most abundant quartz type, whereas polycrystalline quartz is mostly sedimentary and diffuse with more than three grains, altough minor polygonal quartz was also identified. The feldspar contents in the samples varies between 7% - 10%, and it relates to K-feldspar that may include perthitic texture and is altered to sericite or carbonates. The volcanic lithics are felsic and contain quartz and feldspar, the plutonic ones are also felsic by include muscovite (**Figure 6**), the sedimentary ones are laminated mudstones, quartz-rich and k-feldspar rich sandstones, and the metamorphic lithics are mainly muscovite schists (**Figure 6**). Flexed muscovites and biotites were observed in proportions smaller than 5%. Other minerals such as zircon, epidote, chlorite, glauconite and diopside are present in a proportion below 1%. Cements are ferruginous and siliceous (1% - 5%) and it is also common to find organic matter and small sheets of coal partially covering pores.

Sandstones from the upper member varies from coarse to very fine grain, with sub rounded to rounded grains, and high and low sphericity, with moderate to good selection. Contacts between the grains are predominantly concave-convex and sutured, with minor angential contacts. The matrix varies between 4% and 11%, and is dominated by clay in sheet arrangements (**Figure 5**) that corresponds to kaolinite (**Table 1**).

Sandstones are very quartz rich (> 85%) and are classified as sublitharenite and subarkose ([61]; **Figure 6**). Monocrystalline quartz with undulatory extinction is the most abundant quartz type, followed by sedimentary and diffuse polycrystalline quartz with

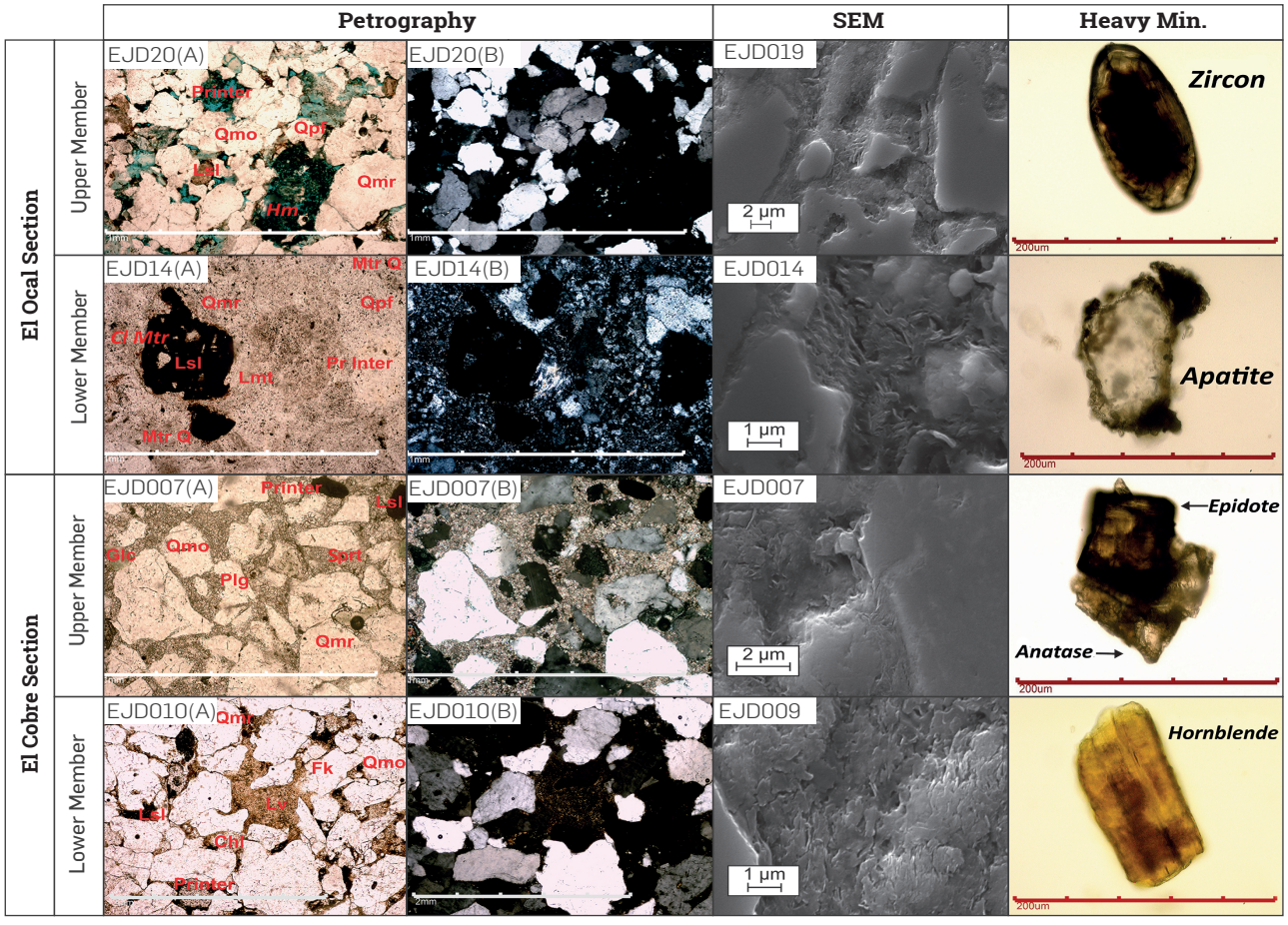

Figure 5. Images relating to petrography, SEM and Heavy Minerals for different samples of each Lower and Upper member of the Caballos Formation, in each study area. Qmr and Qmo = monocrystalline quartz with a straight and wave extinction, respectively, Qpf = polycrystalline quartz with 2 (+2) or more grains (> 10), Fk = Potassium feldspar, Plg = plagioclase, Lv = acidic volcanic lithics, Lsl = sedimentary mudstone lithics, Cht = chert, Cl Mtr = Clay Matrix, Glc = Glauconite, Mo = Organic matter, Hm=Heavy Minerals, Printer = intergranular pores, Printra = intragranular pore, Prfract = Fracture pores. SEM Figure EJD009 (Image in Gray) shows kaolinite-like clays in leaf-like arrangements.

Table 1. Composition, porosity, permeability and X-ray diffraction from the upper and lower members of the Caballos Formation, in the Cobre and Ocal Creeks.

Section	Member of Caballos Formation	Sample	Quartz (%)	Feldespar (%)	Lithiscs (%)	Matrix (%)	Cement (%)	Porosity Average (%)	Permeability K(mD)	Sample	DRX Mineral Phases	DRX (%)
El Ocal	Upper Member	EJD001	98.22	0.81	1.08	11.25	10.75	5.5	0	EJD007	Calcite	26.4
		EJD007	92.99	4.06	0.48	11.52	6.91	5	0		Illite-Smectite	19.7
	Lower Member	EJD009	86.67	4.65	4.65	18.6	3.26	11.4	334.25		Quartz	11.7
		EJD010	85.62	3.66	6.86	17.16	6.18	14.98			Illite	10
		EJD011	97.04	0.54	1.89	3.51	3.78	10.49			Caolinite 1A	6.9
		EJD012a	84.74	5.49	6.73	10.72	6.23	24.01		EJD009	Caolinite 1A	42.1
El Cobre	Upper Member	EJD019	92.74	2.3	3.22	10.11	5.29	29.05	273.4		Quartz	26.5
		EJD020	91.61	1.32	5.53	3.68	2.37	26.9	3.7		Illite-Smectite	10.4
		EJD030	78.14	10.51	4.3	7.69	2.56	4.875		EJD019	Quartz	67.3
		EJD031	82.46	10	2.75	11.25		5.905			Microcline	8.6
		EJD032	90	5.5	1.25	5	14.25	2.575			Caolinite 1A	5.1
	Lower Member	EJD014	78.21	2.39	11.72	10.29	3.83	3.08	0	EJD014	Quartz	51.9
		EJD014A	75.49	7.75	12.5	16.5	1.5	11.31	0.43		Illite-Smectite	16.9
		EJD014C	68.77	2.38	5.24	8.81	4.76	16.98			Caolinite 1A	4.9
		EJD033	83.75	5.71	4.76	17.38	0.71	7.81			Sillimanite	5.1

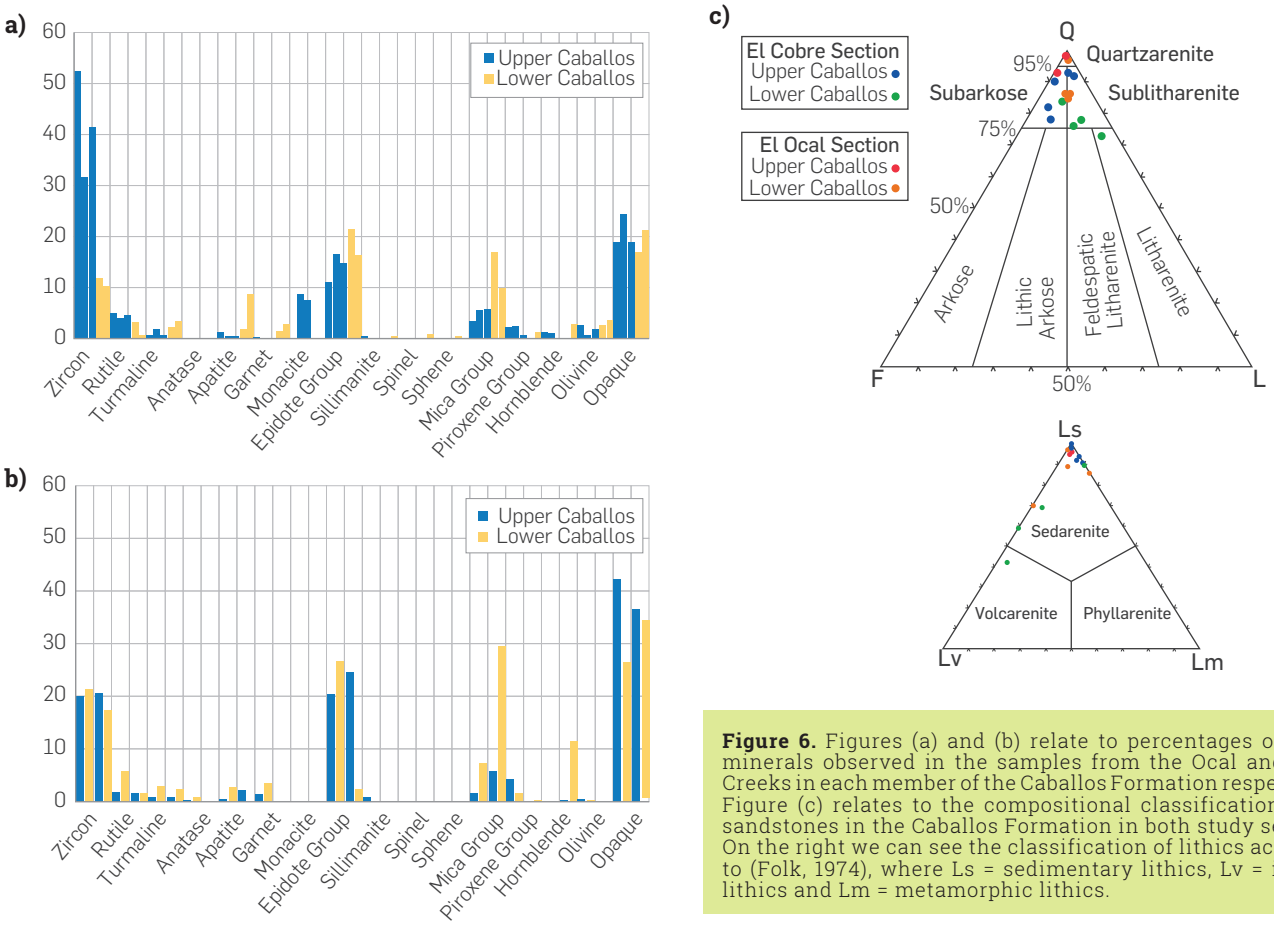

Figure 6. Figures (a) and (b) relate to percentages of heavy minerals observed in the samples from the Ocal and Cobre Creeks in each member of the Caballos Formation respectively. Figure (c) relates to the compositional classification of the sandstones in the Caballos Formation in both study sections. On the right we can see the classification of lithics according to (Folk, 1974), where Ls = sedimentary lithics, Lv = igneous lithics and Lm = metamorphic lithics.

more than three grains. Feldspar varies between 2% -15%, and include mainly K-feldspar with perthitic texture and plagioclase. Lithic fragments include felsic volcanics microcrystalline quartz, mudstone, chert, quartz-rich sandstones and sandstones rich in potassium feldspar. Metamorphic lithics include muscovite schists. Flexed muscovite, biotite, hornblende and zoisite have values below 5%. Other minerals such as zircon, epidote, chlorite, glauconite, titanite and diopside are present in a proportion less than 1%.

Siliceous and calcareous cements were identified (1%-6%). It was common to find organic matter and small remnants of crude oil that partially covering pores, and is usually accompanied by heavy minerals such as epidote, tourmaline, anatase and pyrite.

HEAVY MINERALS

EL OCAL SECTION:
The most abundant ultrastable mineral in the lower member is zircon, followed by rutile and tourmaline (**Figure 5**). Moderately stable and stable minerals include garnets (colorless to reddish), monazites, apatite and titanite. Unstable to highly unstable minerals include zoisite, clinozoisite, epidote, hornblende, diopside, augite, olivine, sphalerite and enstatite in very low proportions (**Table 2**). Opaque minerals vary between 18-24%.

In the upper member, the most abundant mineral is also zircon, followed by rutile and tourmaline (**Figure 5**). Moderately stable and stable minerals include garnet, apatite and, to a lesser extent titanite and sillimanite. Ustable minerals and highly unstable minerals include zoisite, clinozoisite, epidote and muscovites (**Table 2**). Opaque minerals are 17% in abundance.

EL COBRE SECTION:
The most abundant mineral in the lower member is zircon, followed by rutile and tourmaline (**Figure 5**). Moderately stable minerals include garnet, apatite, muscovite and sillimanite (**Figure 5**), while unstable minerals include zoisite, clinozoisite and epidote. The opaques vary between 36-42%. In the upper member the most significant mineral is zircon, followed by rutile and tourmaline (**Figure 5**). Moderately stable and stable minerals include garnets, muscovite and apatite (**Table 2**).

Unstable and highly unstable minerals include zoisite, clinozoisite, epidote, biotite and hornblende. Other heavy minerals found in smaller amounts are diopside, hypersthene, olivine and, monazite (**Table 2**). Opaques vary between 26-33%.

DETRITAL ZIRCON U-Pb GEOCHRONOLOGY

One hundred and fifteen grains of a sublitharenite (**EJD010**) from the lower member in the Ocal Section were analyzed (**Figure 7**). The zircons are mainly sub-rounded with minor prismatic grains. The most significant age populations are Mesoproterozoic (1000-1200 Ma) and Middle Jurassic (172 Ma) (**Figure 7**). Other less-abundant populations are of ages greater than 1500 Ma.

Table 2. Results for the standard analysis on heavy minerals (percentage). The counts were between 370 and 380 grains, including opaque minerals.

	Section	Ocal					Cobre			
	Member	Lower			Upper		Lower		Upper	
	Sample	EJD009	EJD010	EJD012a	EJD001	EJD007	EJD014	EJD014a	EJD019	EJD020
Ultrastable (%)	Zircon	52.53	31.64	41.51	10.44	11.89	20.00	11.89	21.32	17.30
	Rutile	5.07	4.02	4.58	0.78	3.24	1.89	1.62	5.79	1.62
	Tourmaline	0.80	1.88	0.81	3.39	2.43	0.81	0.81	2.89	2.43
	Anatase	0	0	0	0	0	0.2695	0	0.7895	0
Stable (%)	Apatite	1.33	0.54	0.54	8.88	1.89	0.54	2.16	2.89	0.00
	Garnet	0.27	0.00	0.00	2.87	1.62	1.35	0.00	3.42	0.00
	Monazite	0.00	8.85	7.55	0.00	0.00	0.00	0.00	0.79	0.00
Moderately Stable (%)	Sillimanite	0.53	0.00	0.00	0.52	0.00	0.81	0.00	0.00	0.00
	Spinel	0.00	0.00	0.00	1.04	0.00	0.00	0.00	0.00	0.00
	Sphene	0.27	0.00	0.00	0.52	0.27	0.00	0.00	0.00	0.00
Unstable (%)	Epidote	5.07	6.97	3.50	0.52	1.62	8.38	11.62	5.00	0.54
	Zoisite	4.00	5.09	7.28	4.18	15.14	9.73	9.73	16.58	1.35
	Clinozoisite	2.13	4.56	4.04	11.75	4.86	2.16	3.24	5.00	0.54
	Biotite	0.00	0.00	0.00	3.92	6.22	0.00	0.00	0.26	27.57
	Muscovite	3.47	5.63	5.93	6.01	10.54	1.62	5.68	7.11	1.35
	Sericite	0.00	0.00	0.00	0.00	0.27	0.00	0.00	0.00	0.00
	Chlorite	0.00	0.00	0.00	0.00	0.00	0.00	0.00	0.00	0.54
	Augite	0.53	0.00	0.00	0.00	0.00	0.00	0.00	0.00	0.00
	Diopside	1.07	2.41	0.81	0.52	0.00	3.51	0.00	1.32	0.27
	Enstatite	0.27	0.00	0.00	0.00	0.00	0.00	0.00	0.00	0.00
	Hypersthene	0.00	0.00	0.00	0.26	0.00	0.00	0.00	0.26	0.00
	Hornblende	0.00	1.34	1.08	2.87	0.00	0.00	0.27	0.00	11.35
	Olivine	2.67	0.80	1.89	3.66	2.70	0.54	0.00	0.26	0.00
	Sphalerite	0.00	0.27	0.00	0.00	0.00	0.00	0.00	0.00	0.00
Other (%)	Calcite	1.07	0.00	0.27	7.57	5.14	0.27	0.00	0.00	0.00
	Dolomite	0.00	0.00	0.54	1.31	0.54	0.00	0.00	0.00	0.00
	Siderite	0.00	1.61	0.81	5.74	11.08	6.22	7.84	0.53	1.35
	Glauconite	0.00	0.00	0.00	1.83	3.51	0.00	0.00	0.00	0.00
	Opaque	18.93	24.40	18.87	21.41	17.03	42.16	36.49	26.58	33.78

From the upper member one hundred and nineteen zircons were analyzed (quartz arenite EJD007). Most of the zircons are reddish, sub-rounded to prismatic, with low sphericity. The most significant age populations are Mesoproterozoic with peaks at 1020 Ma, 1143 Ma, 1489 Ma and 1586 Ma (**Figure 7**).

In the El Cobre section one hundred thirty-three zircons from a sublitharenite sample (EJD014) were analyzed. The grains are predominantly colorless to oxidized, with elongated and sub-hedral shapes, and minor sub-rounded zircons. The most significant age population is from the Middle Jurassic 171 Ma, with a minor Mesoproterozoic 1000 Ma age population (**Figure 7**).

In a quartz arenite sample (EJD020) from the upper member in Cobre the analyzed one hundred eleven zircons are mainly sub-rounded with low sphericity and prismatic forms. Most zircons are colorless and occasionally appear oxidized with reddish colors. The most significant age populations are defined of Permian (272 Ma), and Upper Jurassic (162.9 Ma). There are less statistically representative peaks of Mesoproterozoic age with ages from 1140 Ma to 1500 Ma.

A ca. 87 Ma single zircon grain was also found. This age is statistically limited (single grain), and is younger than the accumulation age proposed for the Caballos Formation (Aptian - Albian) (**Figure 7**), and is therefore considered as related to lead loss.

DIAGENESIS

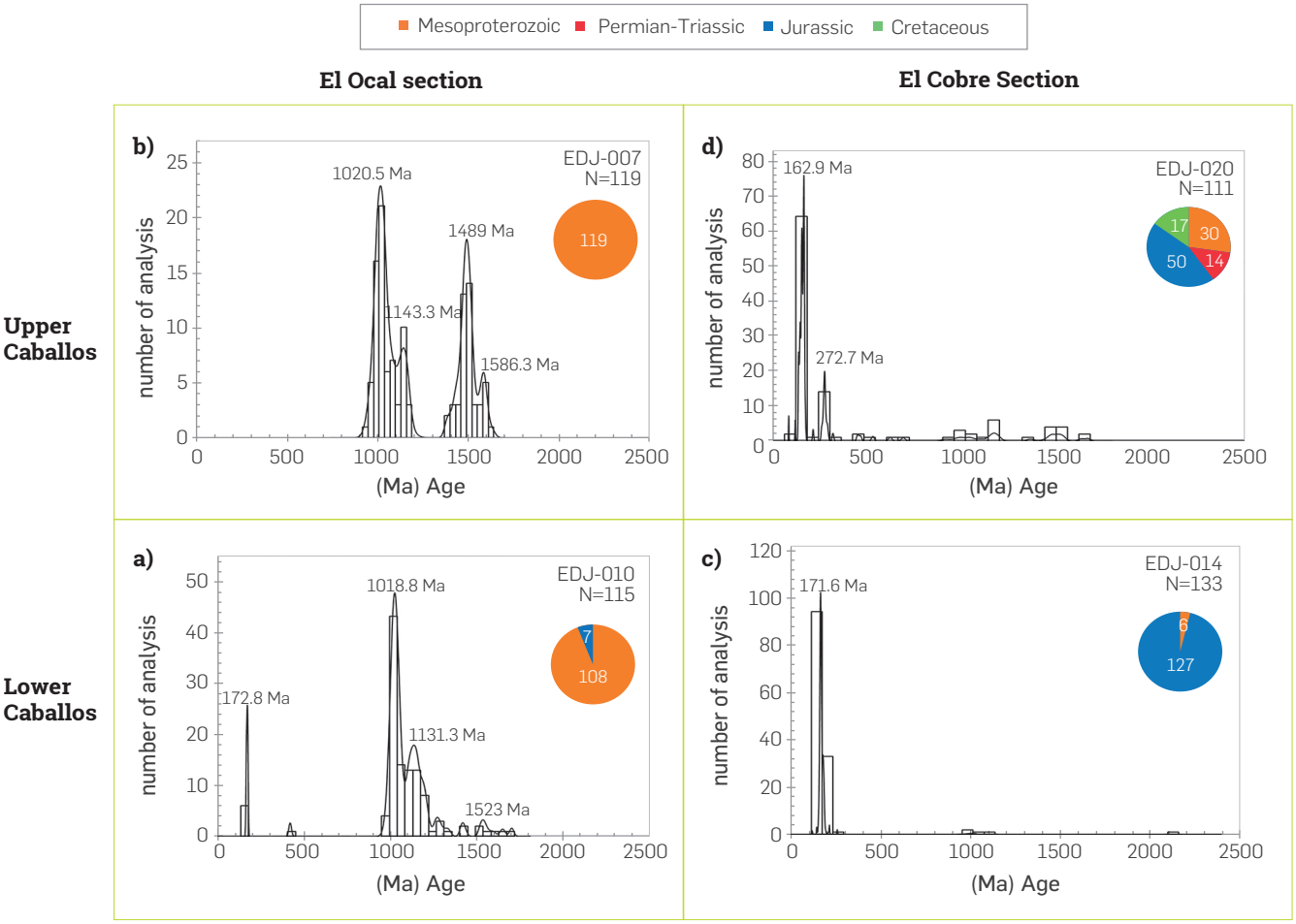

Figure 7. Histograms on frequency and probability distribution for detrital zircons in the samples in the sections studied. Figures (a) and (b) represent the frequencies for the lower and upper members, respectively, in the Ocal section. Figures (c) and (d) relate to the frequencies for the lower and upper members, respectively, of the Caballos Formation in the Cobre section.

The diagenetic characteristics of the Caballos Formation are described below. Given the similarities found in the two studied sections, results are grouped by member.

In the lower member, mechanical compaction includes deformed muscovite as well as muscovite schist, mudstone and volcanic lithics, that also formed a pseudo-matrix. Although samples show different types of contacts, sutured contacts in quartz grains are associated to pressure solution.

K-feldspar, volcanic and sedimentary lithics exhibit partial dissolution. In the El Ocal section the dissolution processes are advanced, with feldspar and quartz crystals characterized by a bay habit.

Primary porosity is intergranular, whereas the secondary is of intragranular and fracture character, the later locally filled with clay and organic material.

Cements are commonly surrounding grains or occluding [62]. The most abundant cement is epitaxial siliceous (opal and chert), the former is found as coats at the the edge of the grains, where the later occludes the porous space. Ferruginous cement is less abundant, and it cover the grains in a thin film, or is found as an intra-matrix pigment, arranged as powder and partially or totally occluding the porous space.

The least common cement is calcareous cement, which fully or partially surrounds the grains in a poikilotopic texture, that locally develops incipiently as sparite. The calcareous cement is also found filling pre-existing fractures in minerals such as quartz.

The upper member includes both pure siliciclastic and mix calcareous-siliciclastic sandstones. The mixed siliciclastic and calcareous rocks are characterized by quartz and feldspar with corrosion bays. On the other hand, the siliciclastic rocks exhibit slightly flexed moscovites and sedimentary lithics, and pressure solution in sutured quartz.

Dissolution is present on grains of feldspar, plagioclase, as well as in the limestone cement, in some grains of glauconite and also in quartz grains and mudstone lithics. Some fragments of mudstone and feldspars are also found as islands. Some of the k-feldspars grains are replace by micrite carbonates and fine clays.

In the siliciclastic rocks porosity is mainly intergranular, with

additionally fracture and dissolution related porosity. In the mixed rocks, the secondary intragranular and fracture porosity predominates, with additional glauconite dissolution and less common intergranular porosity.

Calcareous cement is the most abundant in the mixed rocks, which is present fully or partially surrounding the grains in a poikilotopic texture. It is mainly sparitic, although it´s also found as micrite with a syntaxial texture filling pre-existing fractures in quartz.

The most common cement in siliciclastic samples is of siliceous composition (1-4%), which is found as non-continuous syntax opal along the entire edge of the grains, whereas chert cement is found as an occluding agent. Ferruginous cement (1-3%) is present as a film in the grains and as an intra-matrix pigment, partially or totally occluding the porous space. A summary of the main diagenetic processes that affect the Caballos Formation is presented in Figure 8.

PETROPHYSICAL ANALYSIS

The lower member from the El Ocal section has porosity values between 14-24%, which are greater than those obtained in the upper member (5-6%; Table 2). In the El Cobre section, porosity increases from base to top in the lower member (3-17%), similar to the upper member that varies between 3% and 29%.

The permeability results from El Ocal Section show values of 334.25 md, while for the upper member the permeability results were near zero values. In the El Cobre section, the lower member exhibits low values of 0.43 md, while the upper member varies from 273.4 md to 3.7 md from the base to the top (Table 2).

5. RESULTS ANALYSIS

PROVENANCE

In the two analyzed sections the lower member of the Caballos Formation is characterized by the abundance of monocrystalline quartz of a straight and ondulatory extinction, as well as by the presence of sedimentary and diffuse polycrystalline quartz with more than three grains and feldspar. Lithics include micaceous schists, volcanic, plutonic, mudstone and chert. This suggests a mixed sedimentary, felsic to intermediate igneous and metamorphic lithics of low to medium grade, and short residence time and rapid burial conditions.

The high content of ultrastable phases such as zircon, rutile and tourmaline is likely associated with the recycling of sedimentary rocks, while the presence of garnet, muscovite, sillimanite, pyroxene, hornblende and olivine is likely associated with meta pelitic sources and basic rocks.

The high content of quartz is likely associated with recycled sedimentary sources, as well as a contribution of igneous and metamorphic rocks in conditions of high weathering, as suggested by the relatively high argillaceous matrix contents (6%- 12%).

The upper member from both sections is characterized by an increase in the proportion of quartz (> 93%), and an associated decrease in monocrystalline quartz of straight extinction, at the expense of an increase in quartz with ondulatory extinction, and the appearance of polycrystalline polygonal quartz with 2 to 3 grains, and feldspars (orthoclase, microcline and plagioclase). The lithics are mainly of a sedimentary nature, with minor volcanic and schist lithics.

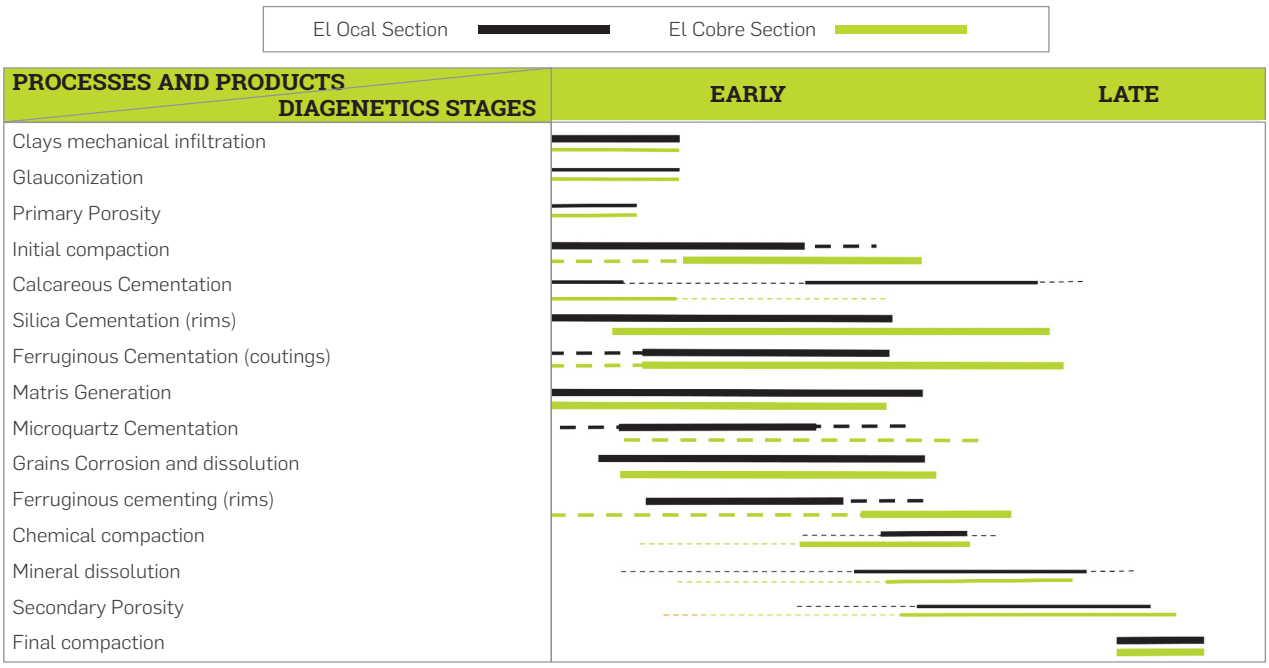

Figure 8. Diagram expressing the sequentiality of the diagenetic events for the Caballos Formation in both study sections. Note the importance of calcareous cementation in the samples analyzed for the Ocal section, which is distinct from what happened in the Cobre section, where siliceous cementation principally dominates. In the Cobre section, the dissolution associated with feldspars seems to have a greater effect on the porosity than for the Ocal section.

These characteristics also suggest mixed source areas. However, metamorphic sources should be of a higher grade, as suggested by the presence of polygonal quartz and feldspars.

The presence of ultra-stable minerals is also compatible with crystalline and recycled sources, while the presence of apatite, garnet, micas, epidote, hornblende, olivine and pyroxenes is also an indicator of basic to acidic crystalline sources.

The compositional characteristics of the lower member in the Ocal Creek, together with the presence of Precambrian and Jurassic detrital zircons in the lower member, suggest that the source areas have characteristics that can be related to exposed rocks, to the east, similar to those present in the Garzón massif, Serranía de La Macarena and the Putumayo region, which include Mesoproterozoic metamorphic rocks of similar ages [19,20] and may be part of the broader Vaupes Arch, as well as Lower Paleozoic siliciclastic rocks (Sedimentitary rocks of Cerro Neiva, El Higado Formation, the Limestones and Sands of Batalla, and the Güejar Group [63]. The volcanic lithics and probably some of the quartz with a straight extinction, together with a population of Jurassic zircons could be related to plutonic or volcanic sources that are also exposed in the eastern segment of the Garzón Massif and the Upper Magdalena Valley [21,64].

The provenance change between the lower and upper members in the Ocal Creek section, which includes the absence of zircons from Jurassic sources and the great abundance of Precambrian zircons, as well as an apparent increase in quartz, including additions of higher-grade metamorphic rocks, could be reflecting a normal denudation process, in which rocks from higher levels of the crust disappear (such as volcanic and sedimentary cover), and crystalline rocks formed in deeper levels are exposed. The proportion of quartz material and the presence of sedimentary material suggests an increase in sources of sedimentary affinity, which could be associated with a migration to the east of the source area, in which Jurassic sources located in the westernmost area -similar to those present in the Garzón Massif and in the Upper Magdalena Valley- would cease to be significant, and are replaced by more eastern sources (**Figure 9**), such as those that are exposed towards the easternmost segments of the Garzón Massif and the Macarena region, where Precambrian gneissic rocks and Paleozoic sedimentary rocks are exposed [20].

In the case of the Cobre Creek, the compositional characteristics and detrital populations also indicate a significant change between the lower and upper members. For the lower member, the extensive Jurassic population and the presence of clastic material of igneous affinity suggest that rocks similar to those exposed in the Upper Magdalena Valley or the Central Cordillera [35] would be the source areas. The sedimentary contribution could be related both to the reworking of the Paleozoic sedimentary rocks exposed on the eastern flank of the Central Cordillera towards the Magdalena Valley, as well as the Jurassic sedimentary rocks associated with the volcanic rocks from the Saldaña Formation, as suggested by the presence of sandstone lithics with feldspar. In the upper member, the appearance of more quartz sources, as well as the presence of Permian and Precambrian zircons, could also be associated with a change in the source area, likely more localized to the west (**Figure 9**), where metamorphic Permo-Triassic rocks and Paleozoic sedimentary rocks are likely exposed [35].

This pattern of denudation change from proximal to more distal source areas, that is also associated to the exposure of deeper crustal levels (**Figure 9**) is characteristic of an extensional environment in which the adjacent topography is being eroded trough time [65]. Intra-basin topographic highs have been identified in the Upper Magdalena Valley as transversal zones in the Neiva sub-basin [66] and is seismic lines [4,5], that were possibly exposed and reduced as the basin deepened and erosion exhausted the topographic highs. Such tend suggest that the generation of topography and tectonic instability would have already been reduced among the upper and lower members of the Caballos Formation (**Figure 10**), thus marking the end of the tectonic instability of the Lower Cretaceous.

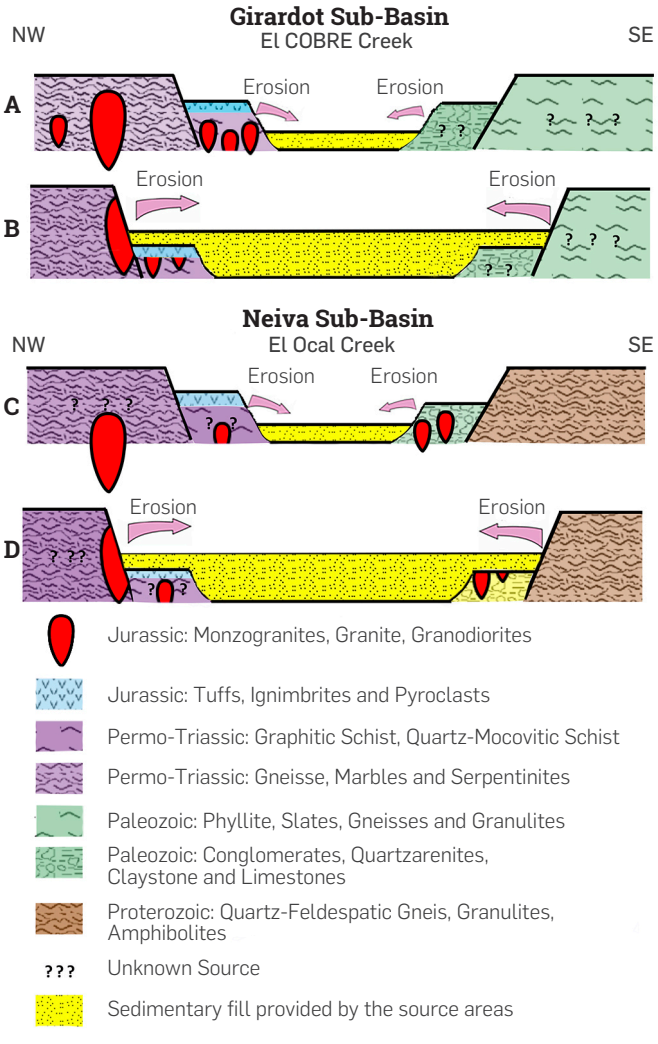

Figure 9. Graphical representation of the lateral denudation and exhumation of deeper blocks in an extensional environment for the study areas. Section A relates to the initial condition (denudation of Jurassic sources) for the Cobre section, which gives rise to the sedimentary fill (yellow). Section B related to the condition after the lateral denudation of the proximal sources for the Cobre section, which gives rise to the w sedimentary fill (yellow) (denudation of Permo-Triassic sources). Section C relates to the initial condition (denudation of Jurassic sources) for Ocal section, which gives rise to the sedimentary fill (yellow). Section D relates to the condition after lateral denudation of the proximal sources for the Ocal section, which gives rise to the sedimentary fill (yellow) (denudation of Precambrian sources).

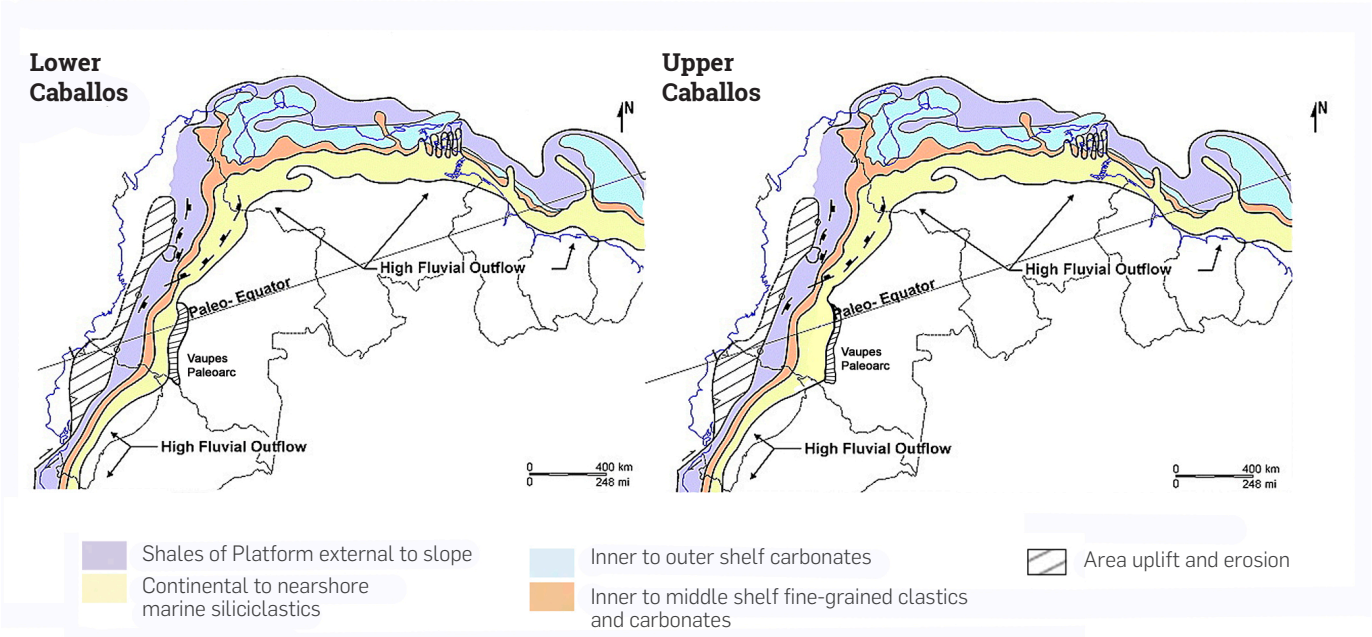

Figure 10. Generalized graphic on the possible paleogeography existing during the Albian-Aptian for the Caballos Formation. Note the decrease in the availability of uplift and erosion area during the deposition of the Upper Member of the Caballos Formation. Modified from [76].

RESERVOIR QUALITY

The Caballos Formation is a proven reservoir in the Upper Magdalena Valley and Putumayo, with a wide variation in its petrophysical properties, with porosity values below 2% in the northeastern part of the basin, and values of 25% towards the northwestern side [45, 67,6]. Some authors have related this feature to the lateral variation of the sedimentary facies that limit the continuity of the reservoirs [4,5]. Other authors have considered the presence of carbonate allochemicals and their relation with the basin's temperatures as a determining factor for the variations in the reservoir's properties in the eastern sector of the basin [6].

Additional petrological controls of reservoir quality includes the primary depositional texture (grain size and selection) and the original composition of the rock and the burial history.

Although grain size and selection influenced reservoirs [68], we didn't found any relation between the petrophysical properties and such attributes.

In the lower and upper members of the Caballos Formation quartz rich rocks are characterized by higher porosity values when compare with those that have higher feldspar and lithics contents with lower quartz contents (Figure 11).

Qualitative and computational diagenetic models [69] suggest that the presence of quartz and feldspar cause less compactation for a given lithostatic pressure than the presence of matrix rich sandstones with schistose or even volcanic lithics. Feldspars might be also affected by dissolution, and although they could initially create secondary porosity, they would lead to the development of clay cements or other cements that would inhibit the generation of secondary porosity.

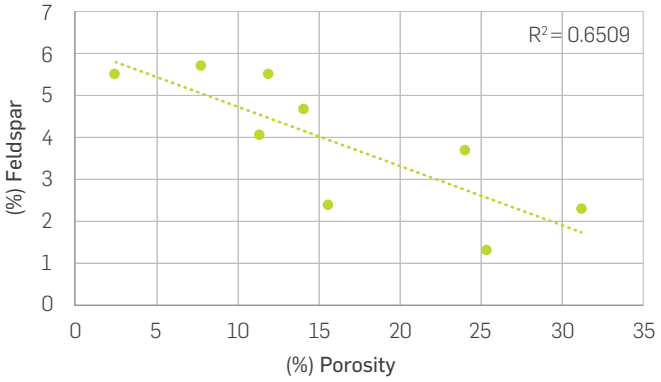

Figure 11. Generalized graphic on porosity vs. feldspar content. The diagram includes samples from both sections and shows the correlation coefficient in the upper right corner. This coefficient seems to indicate a positive correlation between the data plotted.

With the increase in pressure during burial, chemical compaction also tends to increase, with porosity likely decreasing due to the appearance of concave-convex contacts. It is suggested that the lower porosity values are likely associated with the lower member of the Caballos Formation, where the feldspars were probably transformed into clay and a pseudo-matrix was formed due to the compactation of labile volcanic, sedimentary and schistose lithics (Figure 11).

In the upper member of the Caballos Formation, the high porosity and the better permeability values are likely related to feldspar dissolution effects (Figure 11).

Dissolution occurred after burial and development of the siliceous cement, as this cement is cut by both carbonate and ferruginous

cements. It is therefore suggested that this dissolution likely occurred in a late diagenetic state, probably during exhumation, when the chemical interaction with more superficial diagenetic fluids -which would include organic acids- would promote the dissolution of unstable minerals [70,71]. The Caballos Formation was subjected to different deformational phases during the Early Cretaceous, including the orogenic phases of the Albian-Cenomanian and the Cenozoic Andean Orogeny [45,72]. Such episodes promote basin exhumation, causing the development of secondary porosity.

CONCLUSIONS

Provenance results from the Caballos Formation in the Ocal Creek in the southern segment of the Upper Magdalena basins indicates that the source areas include mix sedimentary, acidic to intermediate igneous rocks, and low to medium-grade metamorphic rocks for both the lower and upper memebers of the Formations. These sources exhibit similar characteristics, with those exposed to the east in the Garzón Massif and the Serrania de La Macarena.

In the Cobre Creek, in the northern part of the basin, the sources are mainly igneous and sedimentary rocks that have similarities with the geology of the eastern flank of the Central Cordillera.

The increase in the proportion of quartz, together with the presence of sedimentary material indicate a major change between the lower and upper members. In the Ocal Section it´s suggested that source areas were located farther east whereas for the Cobre section, source areas would probably be located more to the west.

This provenance model is consistent with the extensional model proposed for the Upper Magdalena Valley [1], which suggests that the basin is likely bound by paleo-highs to the east and west and within the basin [73] that were been erode giving place to more distal and deeper crustal sources.

Reservoir quality evaluation suggest that the petrophysical properties of the lower member of the Caballos Formation are controlled by the presence of feldspars and lithics as these components are transformed into clay and produce a pseudo-matrix that reduces the porous space. Whereas in the upper member, the high porosity and the better permeability values are likely related to feldspar dissolution effects during late diagenetic exhumation.

ACKNOWLEDGEMENTS

This work was supported by the joint project "Sinergias en daño de Formación" between ECOPETROL and the Facultad de Minas de la Universidad Nacional de Colombia, Sede Medellín. We would also like to thank the materials laboratory from the Universidad Nacional providing SEM access, and Professor Farid Cortes for facilitating access to XRD analysis. Our thanks go out to the members of the Reservoir Laboratory at Universidad Nacional de Colombia for their support in obtaining the petrophysical results. We thank the members of the EGEO Research Group for their support during different phases of the work. Finally, we would like to express our thanks for the sound comments and suggestions from G. Bayona, R. N. Elrich and an anonymous reviewers who made it possible to improve the this contribution.

REFERENCES

[1] Sarmiento-Rojas, L., Van Wess, J. y Cloetingh, S., Mesozoic transtensional basin history of the Eastern Cordillera, Colombian Andes: Inferences from tectonic models. *Journal of South American Earth Sciences*, 2006, 4 (21), 383-411. https://doi.org/10.1016/j.jsames.2006.07.003.

[2] Villagómez, D., et al., Geochronology, geochemistry and tectonic evolution of the Western and Central Cordilleras of Colombia. *Lithos*, 2011, 3-4 (125), 875–896. https://doi.org/10.1016/j.lithos.2011.05.003

[3] Baby, P.,Rivadeneira, M.,Barragán, R. and Christophout, F., Thick-skinned tectonics in the Oriente foreland basin of Ecuador, in: Nemcok, M., Mora,A. and Cosgrove, J.W.(eds) thick- skin-dominate Orogens, 2013,377.

[4] Duarte, L., Historia de la cuenca cretácea del VSM en un marco crono estratigráfico, Implicaciones Ambientales, *ACGGP Actas 8th Simposio Bolivariano - Exploración Petrolera en las Cuencas Subandinas*, Bogotá, COLOMBIA, pp. 223-232,2003.

[5] Mora, A., Mantilla, M. and De Freitas, M., Cretaceous paleogeography and sedimentation in the Upper Magdalena and Putumayo Basins, Southwestern Colombia, Rio de Janeiro: *AAPG International Conference and Exhibition* 15-18,Bogotá, November 2009.

[6] Mesa, A. G., Diagénesis de la formación Caballos, subcuenca de Girardot: Implicaciones en la calidad del reservorio. Bogotá: *Asociación Colombiana de Geólogos y Geofísicos del Petróleo* (ACGGP), 2004.

[7] Pindell, J. y Dewey, J., Permo-Triassic reconstruction of western Pangea and the evolution of the Gulf of Mexico/Caribbean region, *Tectonics*, 1982, 2 (1), 179-211. https://doi.org/10.1029/TC001i002p00179

[8] Pindell, J., Alleghenian reconstruction and subsequent evolution of the Gulf of Mexico, Bahamas, and Proto-caribbean. *Tectonics*, 1985, 1 (4), 1-39. https://doi.org/10.1029/TC004i001p00001

[9] Cediel, F., Shaw, R. P. and Caceres, C., Tectonic assembly of the Northern Andean Block, in C. Bartolini, R. T. Buffler, and J. Blickwede, eds., The Circum-Gulf of Mexico and the Caribbean: Hydrocarbon habitats, basin formation, and plate tectonics, *AAPG Memoir 79*, (1), 815-848, 2003.

[10] Spikings, R., et al., The geological history of northwestern South America: from Pangaea to the early collision of the Caribbean Large Igneous Province (290–75 Ma). *Gondwana Research*, 2015, 1 (27), 95-139. https://doi.org/10.1016/j.gr.2014.06.004

[11] Martini, M. and Ortega-Gutiérrez, F., Tectono-stratigraphic evolution of eastern Mexico during the break-up of Pangea: A review. *Earth Science Reviews*, 2016. https://doi.org/10.1016/j.earscirev.2016.06.013

[12] Pindell, I. L. and Kennan, W. V., Tectonic evolution of the Gulf of Mexico, Caribbean and northern South America in the mantle reference frame: an update. *Geological Society of London, Special Publication*, 2009, (328), 1 - 56.

[13] Vinasco, C. J., Cordani, U. G., González, H. and Weber, M. C., Geochronological, isotopic, and geochemical data from Permo-Triassic granitic gneisses and granitoids of the colombian Central Andes. *Journal of South American Earth Sciences*, 2006, 4(21), 355-371. https://doi.org/10.1016/j.jsames.2006.07.007

[14] García, R. C., Correa, K., Mantilla, F. L., Bernal, L., Aspectos petrográficos y geoquímicos de las rocas metamórficas del sector barranco de loba (Serranía de San Lucas). *Boletín de Geología de la UIS*, 2009, 1 (31), pp.45-60. ISSN 2145-8553. [Online] Available: http://revistas.uis.edu.co/index.php/revistaboletindegeologia/article/view/165

[15] Bustamante, C., et al., U-Pb LA-ICP-MS geochronology and regional correlation of Middle Jurassic intrusive rocks from the Garzon Massif, Upper Magdalena Valley and Central Cordillera, Southern Colombia. *Boletin de Geología*, 2010, 2 (32), 93-105. ISSN

2145-8553. [Online] Available: http://revistas.uis.edu.co/index.php/revistaboletindegeologia/article/view/2086

[16] Cochrane, R., et al., Distinguishing between in-situ and accretionary growth of continents along active margins. *Lithos*, 2014, (202-203), 382-394. https://doi.org/10.1016/j.lithos.2014.05.031

[17] Nivia, A., Marriner, G. F., Kerr, A. C. and Tarney, J., The Quebrada Grande Complex: a Lower Cretaceous ensialic marginal basin in the Central Cordillera of the Colombian Andes. *Journal of South American Earth Sciences*, 2006, 4 (21), 423 - 436. https://doi.org/10.1016/j.jsames.2006.07.002

[18] Jaramillo, J., Cardona, A., León, S., Valencia, V. and Vinasco, C., Geochemistry and geochronology from Cretaceous magmatic and sedimentary rocks at 6°35´ N, western flank of the Central Cordillera (Colombian Andes): Magmatic record of arc growth and collision. *Journal of South American Earth Sciences*, 2017, (76), 460-481. https://doi.org/10.1016/j.jsames.2017.04.012

[19] Cordani, U. G., Cardona, A., Jimenez, M., Liu, D. and Nutman, A.P., Geochronology of proterozoic basement inliers in the Colombian Andes: Tectonic history of remnants of a fragmented grenville belt, in Vaughan, A.P.M., Leat, P.T., and Pankhurst, R.J., eds., Terrane processes at the margins of Gondwana. *The Geological Society of London, Special Publication* (246), 2005, 329-346. https://doi.org/10.1144/GSL.SP.2005.246

[20] Ibanez-Mejia, M. et al., The Putumayo orogen of Amazonia and its implications for Rodinia reconstructions: New U–Pb geochronological insights into the Proterozoic tectonic evolution of northwestern South America. *Precambrican Research*, 2011, (191), 58-77. https://doi.org/10.1016/j.precamres.2011.09.005

[21] Bustamante, A., Juliani, C., Hall, C. and Essene E., 40Ar/40Ar ages from blueschists of the Jambaló región, Central Cordillera of Colombia: Implications on the styles of accretion in the Northern Andes. *Geologica Acta*, 2011, 3 (9), 351-362. DOI: 10.1344/105.000001697

[22] Harrington, H. and Kay, M., Cambrian and Ordovician faunas of eastern Colombia. *Journal of Paleontology*, 1951, 5(25), 655-668. [Online] Available: http://www.jstor.org/stable/1299905

[23] Stibane, F. and Forero, A., Los afloramientos del Paleozoico en la Jagua (Huila) y Río Nevado (Santander). *Geología Colombiana*, 1969, (6) ,31-66. ISSN electrónico 2357-3767.

[24] Villarroel, C., Macia, C. and Brieva, J., Formación Venado, nueva unidad litoestratigráfica del Ordovícico Colombiano. *Geología Colombiana*, 1997, (22), 41-49. ISSN electrónico 2357-3767.

[25] Mojica, J., Kammer, A. and Ujuet A, G., El Jurásico del sector noroccidental de Suramérica y Guía de la Excursión al Valle Superior del Magdalena Regiones de Payandé y Prado, Departamento del Tolima, Colombia. *Geología Colombiana*, 1996, (21), 3-41. ISSN electrónico 2357-3767.

[26] Moreno-Sánchez, M., L.M., T., Gómez, A. y Ruiz, C., 2016. Formación Nogontova, una nueva unidad litoestratigráfica en la Cordillera Oriental de Colombia. *Boletín de Geología*, 2016, 2 (38), 55-62. https://doi.org/10.18273/revbol.v38n2-2016003.

[27] Sarmiento, L., *Stratigraphy of the Cordillera Oriental west of Bogotá, Colombia*. First ed. (5), 1989, pp.123-139

[28] Moreno, J., Provenance of the Lower Cretaceous sedimentary sequences, central part, Eastern Cordillera, Colombia. *Revista Academia Colombiana de Ciencias Exactas, Físicas y Naturales*, 1991, 69 (18), 159–173. ISSN: 0370-3908.

[29] Fabre, A., Tectonique et generation d'hydrocarbures: un modele de l'evolution de la Cordillere Orientale de Colombie et du Bassin de Llanos pendan le Cretace et le Tertiaire. *Archives des Sciences Geneve*, 1987, (40), 145–190.

[30] Cooper, M. A., et al., Basin development and tectonic history of the Llanos basin, Eastern Cordillera, and Middle Magdalena Valley, Colombia. *American Association of Petroleum Geologists Bulletin*, 1995, 10 (79), 1421-1443.

[31] Gómez, E., et al., Syntectonic Cenozoic sedimentation in the northern Middle Magdalena Valley Basin of Colombia and implications for exhumation of the Northern Andes. *Geological Society of America Bulletin*, 2005, 117 (5-6), 547-569.

[32] Barrio, C. A. and Coffield, D. Q., Late cretaceous stratigraphy of the Upper Magdalena Basin in the Payandé-Chaparral segment (western Girardot Sub-Basin), Colombia. *Journal of South American Earth Sciences*, 1992, 2 (5), 123-139. https://doi.org/10.1016/0895-9811(92)90034-VGet rights and content

[33] Villamil, T., Campanian–Miocene tectonostratigraphy, depocenter evolution and basin development of Colombia and western Venezuela. *Palaeogeography, Palaeoclimatology, Palaeoecology* ,1999, (153), 239–275.

[34] Osorio, C., De Freitas, M., Tellez, G. and Amaral, J., Paleogeography During The Aptian – Albian In The Neiva Subbasin (Upper Magdalena Basin, Colombia). *ACGGP, VIII Simposio Bolivariano-Exploración petrolera en las cuencas subandinas*,Bogotá, COLOMBIA, pp. 331-338, 2003

[35] Bustamante, C., Archanjo, C., Cardona, A. and Vervoort, J., Late Jurassic to Early Cretaceous plutonism in the Colombian Andes: A record of long-term arc maturity. *Geological Society of America Bulletin*, 2016, 11-12 (128), 1762-1779. http://dx.doi.org/10.1130/B31307.1

[36] Etayo-Serna, F., Estudios geológicos del Valle Superior del Magdalena-litoestratigrafía/litología del Cretácico del VSM. Bogotá: Universidad Nacional de Colombia, 1994.

[37] Calderon, J. E., Lithologic prediction from seismic attributes in The Balcon Field, Colombia. *Asociación Colombiana de Geólogos y Geofísicos del Petróleo (ACGGP)*, Bogotá, tercera convención técnica, pp. 12, 2004.

[38] Corrigan, H., The Geology of the Upper Magdalena Basin (northern portion), *Colombian Society of Petroleum Geologists and Geophysicists, Bogotá, Tech. Rep. Geological Field Trips 1958-1978,* pp. 221-251, 1967.

[39] Beltrán, N. and Gallo, J., Guidebook to the geology the Neiva Sub-Basin, Upper Magdalena Basin, southern portion. *Columbian Society of petroleum Geologists and Geophysicists*, Bogotá, (29), pp. 253-273, Field trip of May 31-June 1, 1968.

[40] Sneider, J. S., Depositional enviroment of the Caballos Formation, San Francisco Field, Neiva sub-basin, Upper Magdalena Valley, Colombia. Master's thesis, Texas A&M University, 1988. [Online] Available: http : / /hdl .handle .net /1969 .1 /ETD -TAMU -1988 -THESIS -S6715

[41] Vergara, L., Stratigraphic micropaleontologic and organic geochemical relations in the Cretaceous of the Upper Magdalena Valley,Colombia. Giessener Geologische Schriften,1994, 50 (1),179.

[42] Ramón, J. C. and Fajardo, A., Sedimentología y estratigrafia secuencial de la formación caballos, subcuenca de neiva, valle superior del magdalena. *ACGGP, VIII Simposio Bolivariano-Exploración petrolera en las cuencas subandinas*, Bogotá, COLOMBIA, 2003.

[43] Etayo Serna, F. and Carrillo, C. G., Bioestratigrafía del cretácico mediante macrofósiles en la sección del Ocal, Valle Superior del Magdalena, Colombia. *Geología Colombiana*, 1996, (20), 81-92. ISSN electrónico 2357-3767.

[44] Maher, P.D. and Corrigan, H.T., Generalized composite log of the Ortega Field, Ibagué, Texas Petroleum Co., 1962.

[45] De Freitas, M., Vidal, G. and Mantilla, M., Structural Evolution and Hydrocarbon Entrapment in the Balcon Field. *ACGGP Actas IX Simposio Bolivariano de Exploración en Cuencas Subandinas,* Bogotá, COLOMBIA, pp.253-275,2006.

[46] Powers, M. C., A new roundness scale for sedimentary particles. Sedimentary Petrology, 1953, 2 (23), 117-119. https://doi.org/10.1306/D4269567-2B26-11D7-8648000102C1865D

[47] Ingersoll, V., et al., The effect of grain size on detrital modes: A test of the Gazzi-Dickinson point-counting method. *Sedimentary Petrology*, 1984, 1 (54). http://dx.doi.org/10.1306/212F83B9-2B24-11D7-8648000102C1865D

[48] Basu, A., Young, S. W., Suttner, L. J., James, W. C., Mack, G. H., Re-evaluation of the use of undulatory extinction and polycrystalinity in detrital quartz for provenance interpretation. *Sedimetary Petrology*, 1975, 4 (45), 873-882. http://dx.doi.org/10.1306/212F6E6F-2B24-11D7-8648000102C1865D

[49] Grove, C. and Jerram, D., JPOR: An ImageJ macro to quantify total optical porosity from blue-stained thin sections. *Journal of Computers and Geosciences*, 2011, 11 (37), 1850–1859.

[50] Roduit, N., JMICROVISION, Valle, Ramón, 2007.

[51] Mange, M. A. and Maurer, H., Heavy Minerals in Colour. London: Chapman and Hall, 1992

[52] Chang, Z., Vervoort, J., McClelland, W. and Knaack, C., U-Pb dating of zircon by LA-ICP-MS. *Geochemistry, Geophysics, Geosystems*, 2006, 5 (7), 1-14. https://doi.org/10.1029/2005GC001100

[53] Sláma, J., et al., Plesovice zircon - a new natural reference material for U-Pb and Hf isotopic microanalysis. *Chemical Geology*,2008, 1-2 (245), 1-35. https://doi.org/10.1016/j.chemgeo.2007.11.005

[54] Gehrels, G., Valencia, V. and Pullen, A., Detrital zircon geochronology by laser- ablation multicollector ICPMS at the Arizona LaserChron Center. *Paleontological Society Papers*, 2006, (12), 67–76. https://doi.org/10.1017/S1089332600001352

[55] Ludwig, K., User´s manual for Isoplot 3.7. Berkley, Berkley Geochronology Center, 2007, pp. 70.

[56] Gehrels, G.E., Detrital zircon U-Pb geochronology: current methods and new opportunities, in: Busby, C.J., Azor-Pérez, A. (Eds.), Tectonics of Sedimentary Basins: Recent Advances. Wiley-Blackwell, 2012, pp. 47–62.

[57] Bierman, J. and Kincanon, E., Reconsidering Archimedes' principle. *The Physics Teacher,* 2003, 6 (41) 340-344. https://doi.org/10.1119/1.1607804

[58] Klinkenberg, L. J., The permeability of porous media to liquids and gases, drilling and Production Practice. *American Petroleum Institute*, 1941, API-41-200, 200-213.

[59] Kahle, M., Kleber, M. and Jahn, R., Predicting carbon

content in illitic clay fractions from surface reaction exchange capacity and dithionite-extractable iron. *European Journal of Soil Science*, 2002, (53), 639-644.

[60] Chevron., Proyecto San Luis- Formaciones Payandé, Alpujarra, El Ocal y Caballos Quebrada El Cobre, Bogotá, *Tech. Rep.* M.G.-C.O., 1994.

[61] Folk, R. L., Petrology of Sedimentary Rocks. Austin: Hemphills Eds, 1974, pp.159.

[62] Wilson, M. and Stanton, P., Diagenetic mechanisms of porosity and permeability reduction and enhancement, In : Reservoir Quality Assessment and Prediction In clastic Rocks. *Society Economic Paleontologist and mineralogist Short Course*, (30), 1994, pp. 59-119.

[63] Toussaint, J. F., Evolución Geológica de Colombia. Thesis, *Universidad Nacional de Colombia*, 1993, pp. 229.

[64] Rodríguez, G., Arango, M. I., Zapata, G. and Bermúdez, J. G., Características petrográficas, geoquímicas y edad u-pb de los plutones Jurásico del Valle Superior del Magdalena., *Sociedad Colombiana de Geologia-Bucaramanga*, 2015.

[65] Garzanti, E., Andò, S. and Vezzoli, G., The continental crust as a source of sand (southern Alps crosssection, northern Italy). *Journal of Geology*, 2006, (114), 533–554.

[66] Jiménez, G., Rico, J., Bayona, G., Montes, C., Rosero, A. and Sierra, D., Analysis of curved folds and fault/fold terminations in the southern Upper Magdalena Valley of Colombia. *Journal of South American Earth Sciences*, 2012, (39), 184-201. https://doi.org/10.1016/j.jsames.2012.04.006

[67] González, M., Umaña R., Cruz L.E., Vásquez, M., Informe ejecutivo evaluación del potencial hidrocarburífero de las cuencas colombianas, ANH-UIS, Bogotá, *Tech. Rep. Contrato interadminastrativo nº 2081941 de 2008 fonade-uis-anh*, pp.83-88, 2009.

[68] Roger, M. S., "Chapter 5: Geologic controls on reservoir quality", in: *Handbook of Petroleum Exploration and Production*, Elsevier, 2006, pp. 159-202.

[69] Tobin, R. and Schwarzer, D., Effects of sandstone provenance on reservoir quality preservation in the deep subsurface: experimental modelling of deep-water sand in the Gulf of Mexico. *Geological Society of London, Special Publications*, 2013, (386), 27-47. https://doi.org/10.1144/SP386.17

[70] Guilbaud, R., et al., On the influence of diagenesis on the original composition of Miocene-Pliocene fluvial sandstone in the Himalayan foreland basin of western Nepal. *Journal of Asian Earth Scienes*, 2012, (44), 107-116. DOI: 10.1016/j.jseaes.2011.04.025.

[71] Parnell, J., The role of diagenesis and depositional facies on pore system evolution in a Triassic outcrop analogue (SE Spain). *Marine and Petroleum Geology*, 2015, 51, 136-151. https://doi.org/10.1016/j.marpetgeo.2013.12.004

[72] Anderson, V., et al., Andean topographic growth and basement uplift in southern Colombia, implications for the evolution of the Magdalena, Orinoco, and Amazon River systems, *Geosphere*, 2016, 4 (12), 1235-1256. http://dx.doi.org/10.1130/GES01294.1

[73] Jiménez, G., Rico, J., Bayona, G., Montes, C., Rosero, A. and Sierra, D., Analysis of curved folds and fault/fold terminations in the southern Upper Magdalena Valley of Colombia. Journal of South American Earth Sciences, 2012, (39), 184-201. https://doi.org/10.1016/j.jsames.2012.04.006

[74] Gómez, J., et al., Notas explicativas: Mapa Geológico de Colombia. *Publicaciones Geológicas Especiales 33*, Bogotá (Cundinamarca): Servicio Geológico Colombiano, 2015

[75] Vergara, L., Guerrero, J., Patarroyo, P. and Sarmiento, G., Comentarios acerca de la nomenclatura estratigráfica del Cretácico Inferior del Valle Superior del Magdalena. *Geologia Colombiana*, 1995, (19),21-31. ISSN electrónico 2357-3767.

[76] Erlich, R. N., Villamil, T. and Keens-Dumas, J., Controls on the deposition of Upper Cretaceous organic carbon–rich rocks from Costa Rica to Suriname. *AAPG Memoir*, (79), 1–45, 2003.

ANNEXES

A1. GEOCHRONOLOGICAL DATE

Sample	U	Th	238U	1 sigma	207Pb	1 sigma	206/238 (^{207}corr)	1 sigma	207/206	1 sigma	Best age	1 sigma
Name	ppm	U	206Pb	% error	206Pb	% error	age	abs err	age	abs err		abs err Ma
PUBLICATION TABLE												
EJ D-020_1	327	0.56	44.2796	1.57 %	0.0483	2.73 %	144.0	2.2	115.4	63.2	144.0	2.2
EJ D-020_2	702	0.69	41.7391	1.54 %	0.0493	1.49 %	152.6	2.3	160.1	34.4	152.6	2.3
EJ D-020_3	321	1.00	41.6755	1.49 %	0.0469	2.31 %	152.9	2.2	45.2	54.2	152.9	2.2
EJ D-020_4	842	1.03	39.6679	2.02 %	0.0507	2.78 %	160.5	3.2	228.9	63.0	160.5	3.2
EJ D-020_5	687	0.55	42.5305	1.47 %	0.0496	1.74 %	149.8	2.2	176.6	40.1	149.8	2.2
EJ D-020_6	753	0.81	39.0603	1.44 %	0.0500	1.93 %	163.0	2.3	194.7	44.4	163.0	2.3
EJ D-020_7	859	1.09	41.0293	1.39 %	0.0586	1.39 %	155.2	2.1	551.8	30.1	155.2	2.1
EJ D-020_8	221	0.62	44.4656	1.85 %	0.0608	2.41 %	143.4	2.6	633.5	51.1	143.4	2.6
EJ D-020_9	1,842	1.38	77.5727	1.66 %	0.0509	2.25 %	82.6	1.4	234.8	51.2	82.6	1.4
EJ D-020_10	260	0.45	5.2802	1.27 %	0.0780	0.98 %	1118.1	13.1	1147.3	19.4	1147.3	19.4
EJD-020_11	1,788	0.71	47.2993	1.36 %	0.0510	1.08 %	134.9	1.8	239.4	24.8	134.9	1.8
EJ D-020_12	466	0.74	23.1672	1.45 %	0.0526	1.54 %	272.4	3.9	310.9	34.8	272.4	3.9
EJ D-020_13	1,484	0.49	38.9125	1.28 %	0.0495	1.10 %	163.6	2.1	171.1	25.5	163.6	2.1
EJ D-020_14	609	0.78	41.2307	1.47 %	0.0576	1.56 %	154.5	2.2	514.7	34.0	154.5	2.2
EJ D-020_15	1,208	0.75	3.3560	1.35 %	0.1024	0.75 %	1681.3	20.0	1668.2	13.9	1668.2	13.9
EJ D-020_16	530	0.82	22.6067	1.45 %	0.0595	1.49 %	279.0	4.0	584.5	32.0	279.0	4.0
EJ D-020_17	385	0.73	45.3413	1.57 %	0.0502	2.19 %	140.6	2.2	204.7	50.0	140.6	2.2
EJ D-020_18	518	1.06	41.6342	1.57 %	0.0510	1.64 %	153.0	2.4	241.2	37.5	153.0	2.4
EJ D-020_19	327	0.26	6.2347	1.40 %	0.0715	1.17 %	959.0	12.5	970.5	23.6	970.5	23.6
EJ D-020_20	1,089	1.31	41.0957	1.53 %	0.0500	1.53 %	155.0	2.3	192.9	35.1	155.0	2.3
EJ D-020_21	325	0.56	38.2110	1.53 %	0.0473	2.07 %	166.5	2.5	63.0	48.6	166.5	2.5
EJ D-020_22	726	0.69	44.3706	1.43 %	0.0502	1.37 %	143.7	2.0	202.3	31.4	143.7	2.0
EJ D-020_23	375	0.56	46.8403	1.86 %	0.0496	2.49 %	136.2	2.5	177.5	57.1	136.2	2.5
EJ D-020_24	582	0.63	3.4318	1.43 %	0.1005	0.82 %	1648.5	20.8	1633.1	15.1	1633.1	15.1
EJ D-020_25	410	0.69	24.0928	1.56 %	0.0507	1.60 %	262.2	4.0	225.1	36.5	262.2	4.0
EJ D-020_26	243	0.53	5.8899	1.47 %	0.0738	1.02 %	1010.9	13.7	1037.0	20.4	1037.0	20.4
EJ D-020_27	364	0.96	43.3541	1.49 %	0.0481	2.43 %	147.0	2.2	106.2	56.5	147.0	2.2
EJ D-020_28	485	0.86	44.4930	1.48 %	0.0523	1.79 %	143.3	2.1	297.9	40.4	143.3	2.1
EJ D-020_29	809	1.30	37.3805	1.50 %	0.0498	1.48 %	170.2	2.5	184.9	34.1	170.2	2.5
EJ D-020_30	718	0.46	4.1338	1.37 %	0.0940	0.78 %	1396.6	17.2	1507.7	14.7	1507.7	14.7
EJ D-020_31	322	0.51	5.8968	1.33 %	0.0745	1.04 %	1009.8	12.4	1054.0	20.8	1054.0	20.8
EJ D-020_32	805	0.36	24.5922	1.38 %	0.0528	1.21 %	256.9	3.5	319.0	27.2	256.9	3.5
EJ D-020_33	273	0.47	47.8051	2.02 %	0.0480	2.81 %	133.5	2.7	97.9	65.2	133.5	2.7
EJ D-020_34	299	0.26	3.6887	1.38 %	0.0954	0.89 %	1546.4	19.0	1536.9	16.7	1536.9	16.7
EJ D-020_35	344	0.74	42.6688	1.78 %	0.0484	2.27 %	149.3	2.6	120.0	52.6	149.3	2.6
EJ D-020_36	234	0.54	39.9436	1.86 %	0.0506	2.66 %	159.4	2.9	222.0	60.5	159.4	2.9
EJ D-020_37	614	0.80	22.8931	2.20 %	0.0502	1.92 %	275.6	5.9	205.9	44.0	275.6	5.9
EJ D-020_38	383	0.85	23.1401	1.48 %	0.0542	1.67 %	272.7	4.0	378.9	37.2	272.7	4.0
EJ D-020_39	193	0.54	3.7614	1.37 %	0.0952	1.00 %	1519.7	18.5	1531.8	18.7	1531.8	18.7
EJ D-020_40	573	0.66	38.6458	1.43 %	0.0537	1.53 %	164.7	2.3	360.3	34.2	164.7	2.3
EJ D-020_41	302	0.81	41.9678	1.54 %	0.0491	2.48 %	151.8	2.3	151.2	57.1	151.8	2.3
EJ D-020_42	443	0.53	39.5415	1.46 %	0.0533	2.18 %	161.0	2.3	343.3	48.7	161.0	2.3
EJ D-020_43	412	0.88	23.0398	1.41 %	0.0528	1.48 %	273.9	3.8	319.5	33.2	273.9	3.8
EJ D-020_44	316	0.90	38.8414	1.47 %	0.0491	2.41 %	163.9	2.4	153.3	55.5	163.9	2.4
EJ D-020_45	2,256	0.33	11.7067	1.47 %	0.0609	0.92 %	528.4	7.5	636.6	19.6	528.4	7.5
EJ D-020_46	1,213	0.70	39.4976	1.33 %	0.0491	1.20 %	161.2	2.1	151.2	27.8	161.2	2.1
EJ D-020_47	75	0.83	5.9162	1.44 %	0.0722	1.69 %	1006.7	13.4	992.0	33.9	992.0	33.9
EJ D-020_48	889	0.53	38.8065	1.38 %	0.0503	1.48 %	164.0	2.2	208.3	33.9	164.0	2.2
EJ D-020_49	216	0.44	9.9048	1.57 %	0.0608	1.53 %	620.0	9.3	630.6	32.6	620.0	9.3
EJ D-020_50	463	0.64	38.8576	1.44 %	0.0511	2.13 %	163.8	2.3	244.0	48.4	163.8	2.3
EJ D-020_51	586	0.96	23.2191	1.42 %	0.0519	1.28 %	271.8	3.8	282.7	29.1	271.8	3.8
EJ D-020_52	212	0.71	5.6666	1.45 %	0.0761	0.98 %	1047.7	14.0	1098.7	19.4	1098.7	19.4
EJ D-020_53	1,084	0.86	38.8622	1.39 %	0.0523	1.35 %	163.8	2.3	299.6	30.5	163.8	2.3
EJ D-020_54	416	0.36	4.9529	1.32 %	0.0798	0.89 %	1185.5	14.2	1192.2	17.4	1192.2	17.4
EJ D-020_55	627	0.94	39.8888	2.01 %	0.0872	2.63 %	159.6	3.2	1364.5	49.8	159.6	3.2
EJ D-020_56	1,486	0.18	23.6830	1.48 %	0.0520	1.34 %	266.6	3.9	286.0	30.4	266.6	3.9
EJ D-020_57	480	1.13	3.8305	1.30 %	0.0945	0.95 %	1495.3	17.3	1517.6	17.9	1517.6	17.9
EJ D-020_58	1,058	1.53	47.3013	1.47 %	0.0487	1.34 %	134.9	2.0	133.2	31.3	134.9	2.0
EJ D-020_59	1,478	0.71	42.3549	1.46 %	0.0492	1.21 %	150.4	2.2	156.2	28.2	150.4	2.2
EJ D-020_60	484	0.92	23.1678	1.52 %	0.0526	1.63 %	272.4	4.1	309.6	36.7	272.4	4.1
EJ D-020_61	175	0.63	3.9781	1.60 %	0.0910	1.05 %	1445.6	20.7	1445.8	19.9	1445.8	19.9

Sample	U	Th	238U	1 sigma	207Pb	1 sigma	206/238 (^{207}corr)	1 sigma	207/206	1 sigma	Best age	1 sigma
Name	ppm	U	206Pb	% error	206Pb	% error	age	abs err	age	abs err		abs err Ma
EJ D-020_62	358	0.61	39.7849	1.73 %	0.0469	1.71 %	160.0	2.7	44.4	40.4	160.0	2.7
EJ D-020_63	721	0.19	4.6413	1.49 %	0.0921	0.84 %	1257.8	16.9	1469.0	15.9	1469.0	15.9
EJ D-020_64	550	0.46	5.6557	1.28 %	0.0781	0.95 %	1049.5	12.4	1149.6	18.8	1149.6	18.8
EJ D-020_65	606	0.80	39.8145	1.43 %	0.0509	1.54 %	159.9	2.3	235.9	35.1	159.9	2.3
EJ D-020_66	206	0.60	38.3764	1.97 %	0.0595	3.71 %	165.8	3.2	585.1	78.6	165.8	3.2
EJ D-020_67	341	0.65	22.0534	1.46 %	0.0530	1.44 %	285.9	4.1	330.1	32.4	285.9	4.1
EJ D-020_68	363	0.69	4.9994	1.33 %	0.0797	1.03 %	1175.5	14.3	1190.0	20.2	1190.0	20.2
EJ D-020_69	819	0.78	38.6057	1.33 %	0.0485	1.58 %	164.9	2.2	124.6	36.8	164.9	2.2
EJ D-020_70	1,632	0.96	42.0027	1.29 %	0.0495	1.26 %	151.7	1.9	173.4	29.1	151.7	1.9
EJ D-020_71	321	0.46	6.4387	1.34 %	0.0695	0.99 %	930.7	11.6	913.0	20.2	913.0	20.2
EJ D-020_72	736	0.97	21.7956	1.58 %	0.0525	1.17 %	289.2	4.5	308.6	26.5	289.2	4.5
EJ D-020_73	135	0.52	43.0039	2.96 %	0.0842	4.02 %	148.2	4.3	1297.4	76.2	148.2	4.3
EJ D-020_74	847	1.32	13.9072	1.27 %	0.0621	0.86 %	447.6	5.5	679.1	18.2	447.6	5.5
EJ D-020_75	809	1.07	39.1561	1.36 %	0.0493	1.49 %	162.6	2.2	163.5	34.5	162.6	2.2
EJ D-020_76	682	1.28	42.2248	1.36 %	0.0494	1.58 %	150.9	2.0	168.3	36.4	150.9	2.0
EJ D-020_77	344	0.75	41.0829	1.35 %	0.0499	2.13 %	155.0	2.1	189.4	48.8	155.0	2.1
EJ D-020_78	567	0.82	23.0452	1.27 %	0.0531	1.32 %	273.8	3.4	332.8	29.7	273.8	3.4
EJ D-020_79	963	0.24	3.7302	1.60 %	0.0924	0.87 %	1531.1	21.8	1476.5	16.4	1476.5	16.4
EJ D-020_80	385	0.55	39.4059	1.77 %	0.0478	1.93 %	161.5	2.8	87.2	45.2	161.5	2.8
EJ D-020_81	1,168	0.79	41.2958	1.39 %	0.0500	1.47 %	154.2	2.1	194.0	33.8	154.2	2.1
EJ D-020_82	1,169	0.95	39.7405	1.34 %	0.0508	1.40 %	160.2	2.1	231.0	31.9	160.2	2.1
EJ D-020_83	536	0.82	23.4865	1.40 %	0.0508	1.33 %	268.8	3.7	229.9	30.5	268.8	3.7
EJ D-020_84	256	0.67	3.8298	1.35 %	0.0930	0.85 %	1495.5	18.0	1488.5	16.0	1488.5	16.0
EJ D-020_85	256	0.49	8.8583	1.58 %	0.0643	1.08 %	689.5	10.3	752.8	22.6	689.5	10.3
EJ D-020_86	712	0.62	45.6468	1.53 %	0.0478	1.64 %	139.7	2.1	90.1	38.4	139.7	2.1
EJ D-020_87	864	0.44	42.6642	1.53 %	0.0503	1.17 %	149.4	2.3	208.5	26.8	149.4	2.3
EJ D-020_88	708	0.53	46.5152	1.54 %	0.0484	1.54 %	137.1	2.1	119.5	35.9	137.1	2.1
EJ D-020_89	378	0.54	47.4233	1.61 %	0.0487	2.19 %	134.5	2.1	135.3	50.7	134.5	2.1
EJ D-020_90	617	0.73	39.1172	1.44 %	0.0509	1.34 %	162.7	2.3	235.7	30.7	162.7	2.3
EJ D-020_91	647	0.51	41.2682	1.56 %	0.0518	1.65 %	154.3	2.4	277.5	37.4	154.3	2.4
EJ D-020_92	711	0.63	38.5278	1.56 %	0.0514	1.37 %	165.2	2.5	257.5	31.2	165.2	2.5
EJ D-020_93	305	0.63	13.4497	1.47 %	0.0572	1.52 %	462.3	6.5	497.6	33.1	462.3	6.5
EJ D-020_94	932	0.61	42.8160	1.53 %	0.0508	1.31 %	148.8	2.3	231.7	29.9	148.8	2.3
EJ D-020_95	603	0.53	39.0943	1.52 %	0.0501	1.74 %	162.8	2.4	200.1	40.0	162.8	2.4
EJ D-020_96	292	0.38	4.8966	1.45 %	0.0792	0.88 %	1198.0	15.8	1177.2	17.2	1177.2	17.2
EJ D-020_97	209	0.61	4.4446	1.50 %	0.0871	0.93 %	1308.2	17.8	1363.6	17.8	1363.6	17.8
EJ D-020_98	843	0.44	5.1580	1.43 %	0.0788	0.78 %	1142.3	14.9	1166.0	15.3	1166.0	15.3
EJ D-020_99	259	1.09	37.3209	1.80 %	0.0460	2.40 %	170.5	3.0	0.0	53.7	170.5	3.0
EJ D-020_100	329	0.60	45.1544	1.63 %	0.0508	1.85 %	141.2	2.3	231.1	42.2	141.2	2.3
EJ D-020_101	152	0.61	6.2619	1.83 %	0.0724	1.09 %	955.1	16.2	998.2	21.9	998.2	21.9
EJ D-020_102	473	0.67	19.8523	1.45 %	0.0548	1.35 %	316.8	4.5	403.4	30.0	316.8	4.5
EJ D-020_103	205	0.60	41.6708	1.80 %	0.0500	2.65 %	152.9	2.7	195.4	60.5	152.9	2.7
EJ D-020_104	665	0.84	29.9471	1.43 %	0.0516	1.31 %	211.7	3.0	266.4	29.9	211.7	3.0
EJ D-020_105	822	0.77	42.2928	1.36 %	0.0509	1.71 %	150.6	2.0	237.7	39.1	150.6	2.0
EJ D-020_106	202	0.72	44.4561	1.96 %	0.0489	2.76 %	143.4	2.8	144.3	63.5	143.4	2.8
EJ D-020_107	507	1.03	39.9665	1.66 %	0.0503	1.70 %	159.3	2.6	208.3	38.9	159.3	2.6
EJ D-020_108	491	0.70	40.1341	1.57 %	0.0495	1.89 %	158.7	2.5	172.8	43.4	158.7	2.5
EJ D-020_109	644	0.60	38.3501	1.41 %	0.0485	1.62 %	165.9	2.3	121.7	37.7	165.9	2.3
EJD-020_110	1,103	0.64	54.5173	1.41 %	0.0541	1.45 %	117.2	1.6	373.2	32.4	117.2	1.6
EJD-020 111	196	0.62	44.4663	2.02 %	0.0487	2.55 %	143.4	2.9	132.5	58.8	143.4	2.9
EJ D-007_1	125	0.68	5.9360	1.54 %	0.0724	1.28 %	1003.6	14.3	996.5	25.7	996.5	25.7
EJ D-007_2	160	0.76	3.6494	1.34 %	0.0965	0.91 %	1561.2	18.6	1556.6	17.1	1556.6	17.1
EJ D-007_3	72	0.60	3.6324	1.60 %	0.0966	1.10 %	1567.6	22.2	1559.3	20.5	1559.3	20.5
EJ D-007_4	466	0.46	5.2566	1.31 %	0.0774	0.85 %	1122.7	13.5	1131.5	16.8	1131.5	16.8
EJ D-007_5	254	0.45	4.3909	1.46 %	0.0886	0.85 %	1322.7	17.5	1394.8	16.2	1394.8	16.2
EJ D-007_6	217	0.93	5.8400	1.38 %	0.0732	0.91 %	1018.9	12.9	1020.2	18.3	1020.2	18.3
EJ D-007_7	147	0.38	5.1732	1.40 %	0.0752	1.07 %	1139.2	14.6	1075.0	21.3	1075.0	21.3
EJ D-007_8	156	0.38	5.9965	1.40 %	0.0707	1.16 %	994.3	12.9	949.6	23.6	949.6	23.6
EJ D-007_9	54	0.54	5.5193	1.61 %	0.0751	1.71 %	1073.4	15.9	1070.8	33.9	1070.8	33.9
EJ D-007_10	169	0.64	3.5668	1.40 %	0.0979	0.94 %	1593.2	19.7	1583.7	17.5	1583.7	17.5
EJD-007_11	218	1.65	6.0164	1.40 %	0.0726	0.98 %	991.2	12.9	1003.1	19.8	1003.1	19.8

Sample	U	Th	238U	1 sigma	207Pb	1 sigma	206/238 (^{207}corr)	1 sigma	207/206	1 sigma	Best age	1 sigma
Name	ppm	U	206Pb	% error	206Pb	% error	age	abs err	age	abs err		abs err Ma
EJ D-007_12	127	0.44	5.3927	1.52 %	0.0776	1.62 %	1096.6	15.3	1135.4	32.0	1135.4	32.0
EJ D-007_13	124	0.71	3.5774	1.40 %	0.1001	1.02 %	1589.0	19.7	1626.3	18.9	1626.3	18.9
EJ D-007_14	490	1.24	5.8598	1.35 %	0.0744	0.88 %	1015.7	12.6	1053.5	17.6	1053.5	17.6
EJ D-007_15	146	0.50	5.1243	1.37 %	0.0775	1.08 %	1149.2	14.4	1135.1	21.3	1135.1	21.3
EJ D-007_16	58	0.80	5.8593	1.52 %	0.0739	1.99 %	1015.8	14.3	1038.2	39.6	1038.2	39.6
EJ D-007_17	178	1.40	3.8618	1.39 %	0.0974	0.97 %	1484.4	18.4	1574.5	18.0	1574.5	18.0
EJD-007 18	249	0.43	5.3182	1.35 %	0.0898	0.99 %	1110.7	13.7	1421.4	18.9	1421.4	18.9
EJ D-007_19	195	0.49	5.8840	1.40 %	0.0733	1.16 %	1011.8	13.1	1021.3	23.3	1021.3	23.3
EJ D-007_20	263	0.46	5.7717	1.43 %	0.0713	1.00 %	1030.0	13.6	967.4	20.3	967.4	20.3
EJ D-007_21	253	0.50	3.8651	1.34 %	0.0929	0.89 %	1483.3	17.8	1485.9	16.7	1485.9	16.7
EJ D-007_22	297	0.30	3.8050	1.32 %	0.0939	0.87 %	1504.2	17.7	1506.5	16.3	1506.5	16.3
EJ D-007_23	229	0.73	5.8692	1.32 %	0.0735	1.11 %	1014.2	12.4	1028.0	22.2	1028.0	22.2
EJ D-007_24	269	0.57	3.8007	1.29 %	0.0935	0.93 %	1505.7	17.3	1497.3	17.5	1497.3	17.5
EJ D-007_25	362	0.68	3.6114	1.33 %	0.0980	0.75 %	1575.7	18.6	1586.8	14.0	1586.8	14.0
EJ D-007_26	92	0.54	5.4787	1.58 %	0.0734	1.89 %	1080.8	15.7	1026.2	37.9	1026.2	37.9
EJ D-007_27	737	0.58	5.9347	1.31 %	0.0719	0.82 %	1003.8	12.2	984.3	16.6	984.3	16.6
EJ D-007_28	145	0.48	5.4698	1.33 %	0.0762	1.14 %	1082.4	13.2	1099.2	22.6	1099.2	22.6
EJ D-007_29	674	0.69	5.8416	1.28 %	0.0722	0.80 %	1018.6	12.1	991.6	16.2	991.6	16.2
EJ D-007_30	180	0.58	5.8185	1.43 %	0.0731	1.01 %	1022.4	13.5	1015.6	20.4	1015.6	20.4
EJ D-007_31	577	0.40	4.8624	1.30 %	0.0785	0.84 %	1205.7	14.3	1158.9	16.5	1158.9	16.5
EJ D-007_32	131	0.58	6.0156	1.40 %	0.0732	1.20 %	991.3	12.8	1020.2	24.1	1020.2	24.1
EJ D-007_33	210	0.65	3.8008	1.32 %	0.0944	0.91 %	1505.7	17.7	1515.3	17.0	1515.3	17.0
EJ D-007_34	229	0.64	3.8286	1.32 %	0.0946	0.86 %	1495.9	17.6	1519.3	16.1	1519.3	16.1
EJ D-007_35	456	0.45	5.8545	1.34 %	0.0735	0.86 %	1016.6	12.6	1028.1	17.4	1028.1	17.4
EJ D-007_36	318	0.49	5.9558	1.34 %	0.0725	0.90 %	1000.6	12.4	999.0	18.2	999.0	18.2
EJ D-007_37	306	0.50	3.7928	1.31 %	0.0938	0.82 %	1508.5	17.6	1504.0	15.5	1504.0	15.5
EJ D-007_38	195	0.43	3.7947	1.33 %	0.0933	0.97 %	1507.9	17.9	1493.1	18.2	1493.1	18.2
EJ D-007_39	191	0.71	5.9195	1.36 %	0.0724	0.99 %	1006.2	12.7	996.4	19.9	996.4	19.9
EJ D-007_40	277	0.66	3.7652	1.36 %	0.0978	0.83 %	1518.4	18.3	1583.3	15.4	1583.3	15.4
EJ D-007_41	399	0.49	5.8679	1.37 %	0.0741	0.88 %	1014.4	12.9	1043.5	17.6	1043.5	17.6
EJ D-007_42	390	0.64	3.5128	1.32 %	0.0986	0.79 %	1614.8	18.8	1598.6	14.6	1598.6	14.6
EJ D-007_43	337	0.51	5.7825	1.33 %	0.0734	0.85 %	1028.3	12.6	1026.4	17.2	1026.4	17.2
EJ D-007_44	93	0.70	5.8731	1.43 %	0.0736	1.41 %	1013.6	13.4	1029.9	28.3	1029.9	28.3
EJ D-007_45	156	0.56	3.8260	1.43 %	0.0924	0.96 %	1496.9	19.1	1474.8	18.2	1474.8	18.2
EJ D-007_46	260	0.62	5.0818	1.37 %	0.0787	1.01 %	1158.0	14.5	1164.3	19.9	1164.3	19.9
EJ D-007_47	59	0.78	5.9578	1.45 %	0.0745	1.72 %	1000.2	13.4	1056.1	34.3	1056.1	34.3
EJ D-007_48	307	0.42	4.6356	1.33 %	0.0879	0.82 %	1259.2	15.2	1381.3	15.6	1381.3	15.6
EJ D-007_49	61	1.32	5.8517	1.61 %	0.0744	1.47 %	1017.0	15.1	1052.7	29.3	1052.7	29.3
EJ D-007_50	277	0.42	5.4305	1.35 %	0.0744	0.95 %	1089.6	13.5	1052.2	19.0	1052.2	19.0
EJ D-007_51	122	0.89	5.9739	1.48 %	0.0713	1.30 %	997.7	13.6	966.6	26.3	966.6	26.3
EJ D-007_52	201	0.38	4.9587	1.34 %	0.0779	1.05 %	1184.3	14.5	1145.3	20.8	1145.3	20.8
EJ D-007_53	98	1.02	3.7529	1.35 %	0.0947	1.09 %	1522.8	18.3	1521.9	20.5	1521.9	20.5
EJ D-007_54	470	0.28	5.8862	1.33 %	0.0737	0.82 %	1011.5	12.4	1032.8	16.5	1032.8	16.5
EJ D-007_55	353	0.41	3.7735	1.28 %	0.0936	0.85 %	1515.4	17.3	1499.5	15.9	1499.5	15.9
EJ D-007_56	268	0.46	4.0007	1.36 %	0.0901	0.92 %	1438.3	17.6	1427.7	17.6	1427.7	17.6
EJ D-007_57	171	0.41	5.2758	1.49 %	0.0774	1.01 %	1118.9	15.3	1131.8	20.0	1131.8	20.0
EJ D-007_58	49	0.40	5.6246	1.70 %	0.0765	1.53 %	1054.9	16.6	1107.0	30.3	1107.0	30.3
EJ D-007_59	208	0.52	5.9095	1.32 %	0.0725	1.00 %	1007.8	12.3	1000.2	20.1	1000.2	20.1
EJ D-007_60	189	0.38	3.9137	1.31 %	0.0926	0.84 %	1466.9	17.1	1480.0	15.8	1480.0	15.8
EJ D-007_61	150	0.51	5.4901	1.46 %	0.0753	1.08 %	1078.7	14.5	1077.8	21.5	1077.8	21.5
EJ D-007_62	227	0.22	4.2480	1.36 %	0.0907	0.90 %	1362.8	16.7	1441.4	17.1	1441.4	17.1
EJ D-007_63	220	0.51	5.9011	1.41 %	0.0717	1.12 %	1009.1	13.2	976.8	22.6	976.8	22.6
EJ D-007_64	319	0.38	4.0070	1.46 %	0.0912	0.88 %	1436.2	18.8	1450.3	16.6	1450.3	16.6
EJ D-007_65	260	0.29	3.8077	1.36 %	0.0934	0.89 %	1503.3	18.2	1495.1	16.8	1495.1	16.8
EJ D-007_66	701	0.36	5.8900	1.40 %	0.0728	0.85 %	1010.9	13.1	1007.2	17.0	1007.2	17.0
EJ D-007_67	432	0.49	5.6422	1.30 %	0.0725	0.84 %	1051.9	12.6	1001.2	17.0	1001.2	17.0
EJ D-007_68	565	0.56	5.6776	1.34 %	0.0739	0.76 %	1045.8	12.9	1038.5	15.3	1038.5	15.3
EJ D-007_69	212	0.50	5.2236	1.34 %	0.0783	0.92 %	1129.2	13.9	1153.9	18.2	1153.9	18.2
EJ D-007_70	484	0.40	3.8955	1.29 %	0.0927	0.79 %	1473.0	17.0	1481.2	15.0	1481.2	15.0
EJ D-007_71	122	0.51	3.9607	1.41 %	0.0949	1.02 %	1451.2	18.3	1526.6	19.1	1526.6	19.1
EJ D-007_72	131	0.23	3.7926	1.86 %	0.0957	1.86 %	1508.6	24.9	1541.2	34.5	1541.2	34.5
EJ D-007_73	247	0.66	5.7640	1.44 %	0.0736	1.05 %	1031.3	13.7	1029.2	21.1	1029.2	21.1

Sample	U	Th	238U	1 sigma	207Pb	1 sigma	206/238 (^{207}corr)	1 sigma	207/206	1 sigma	Best age	1 sigma
Name	ppm	U	206Pb	% error	206Pb	% error	age	abs err	age	abs err		abs err Ma
EJ D-007_74	93	0.68	5.7965	1.49 %	0.0727	1.36 %	1026.0	14.1	1005.5	27.3	1005.5	27.3
EJ D-007_75	183	1.15	5.5372	1.34 %	0.0730	1.03 %	1070.2	13.2	1012.9	20.8	1012.9	20.8
EJ D-007_76	327	0.79	3.8455	1.33 %	0.0938	0.85 %	1490.1	17.7	1504.4	16.0	1504.4	16.0
EJ D-007_77	176	0.52	3.8513	1.32 %	0.0924	0.88 %	1488.1	17.5	1475.8	16.6	1475.8	16.6
EJ D-007_78	150	0.54	5.7772	1.33 %	0.0727	1.28 %	1029.1	12.7	1006.9	25.8	1006.9	25.8
EJ D-007_79	160	0.41	3.8389	1.36 %	0.0943	0.89 %	1492.4	18.0	1513.2	16.7	1513.2	16.7
EJ D-007_80	830	0.61	5.9136	1.32 %	0.0735	0.87 %	1007.2	12.3	1026.8	17.4	1026.8	17.4
EJ D-007_81	100	0.50	5.6915	1.42 %	0.0726	1.37 %	1043.4	13.6	1002.9	27.7	1002.9	27.7
EJ D-007_82	693	0.47	5.7045	1.30 %	0.0725	0.80 %	1041.2	12.5	1000.9	16.1	1000.9	16.1
EJ D-007_83	429	0.59	3.9219	1.31 %	0.0927	0.79 %	1464.1	17.2	1480.8	14.9	1480.8	14.9
EJ D-007_84	256	0.48	5.5653	1.29 %	0.0736	0.95 %	1065.2	12.7	1031.3	19.0	1031.3	19.0
EJ D-007_85	271	0.73	3.6484	1.49 %	0.0941	0.89 %	1561.5	20.7	1509.6	16.6	1509.6	16.6
EJ D-007_86	207	0.62	3.8148	1.38 %	0.0931	0.91 %	1500.8	18.4	1489.0	17.1	1489.0	17.1
EJ D-007_87	437	1.12	5.8523	1.33 %	0.0735	0.90 %	1016.9	12.5	1026.4	18.0	1026.4	18.0
EJ D-007_88	154	0.46	3.8204	1.40 %	0.0942	0.93 %	1498.8	18.7	1512.2	17.5	1512.2	17.5
EJ D-007_89	146	0.65	3.8644	1.43 %	0.0921	0.99 %	1483.6	18.9	1469.5	18.6	1469.5	18.6
EJ D-007_90	438	0.52	5.9132	1.33 %	0.0733	0.92 %	1007.2	12.3	1022.1	18.4	1022.1	18.4
EJ D-007_91	284	0.43	4.1499	1.37 %	0.0901	0.85 %	1391.7	17.2	1427.4	16.2	1427.4	16.2
EJ D-007_92	280	0.36	5.2412	1.32 %	0.0790	0.88 %	1125.7	13.6	1171.5	17.3	1171.5	17.3
EJ D-007_93	181	0.42	5.4344	1.33%	0.0753	1.05 %	1088.9	13.3	1075.4	21.0	1075.4	21.0
EJ D-007_94	93	0.52	5.3345	1.56 %	0.0754	1.23 %	1107.6	15.8	1078.4	24.4	1078.4	24.4
EJ D-007_95	190	0.65	3.8942	1.38 %	0.0926	0.88 %	1473.4	18.1	1479.7	16.7	1479.7	16.7
EJ D-007_96	288	0.41	5.8362	1.31 %	0.0744	0.97 %	1019.5	12.3	1053.4	19.4	1053.4	19.4
EJ D-007_97	971	0.53	5.9513	1.38 %	0.0726	0.79 %	1001.3	12.8	1002.3	15.9	1002.3	15.9
EJ D-007_98	189	0.90	5.1683	1.45 %	0.0783	1.04 %	1140.2	15.1	1155.5	20.5	1155.5	20.5
EJ D-007_99	287	0.85	5.5759	1.34 %	0.0738	0.88 %	1063.4	13.1	1037.0	17.7	1037.0	17.7
EJ D-007_100	44	0.48	5.2498	1.66 %	0.0775	1.97 %	1124.0	17.1	1134.3	38.7	1134.3	38.7
EJ D-007_101	94	0.60	5.0554	1.42 %	0.0775	1.35 %	1163.5	15.1	1133.1	26.6	1133.1	26.6
EJ D-007_102	158	0.44	4.0403	1.42 %	0.0918	0.96 %	1425.6	18.2	1464.2	18.1	1464.2	18.1
EJ D-007_103	64	0.26	5.1874	1.68 %	0.0768	1.61 %	1136.4	17.5	1117.2	31.8	1117.2	31.8
EJ D-007_104	103	0.78	3.5135	1.35 %	0.0979	1.03 %	1614.6	19.2	1584.6	19.2	1584.6	19.2
EJ D-007_105	43	0.33	5.1341	1.60 %	0.0794	1.70 %	1147.2	16.8	1182.2	33.3	1182.2	33.3
EJ D-007_106	220	0.62	3.7377	1.42 %	0.0934	0.91 %	1528.3	19.3	1496.1	17.1	1496.1	17.1
EJ D-007_107	303	0.73	5.8327	1.36 %	0.0734	0.95 %	1020.1	12.8	1024.4	19.0	1024.4	19.0
EJ D-007_108	880	0.41	3.8312	1.26 %	0.0926	0.77 %	1495.0	16.8	1480.1	14.6	1480.1	14.6
EJ D-007_109	701	0.17	5.6619	1.35 %	0.0725	0.81 %	1048.5	13.0	1000.8	16.4	1000.8	16.4
EJD-007_110	369	0.45	3.8451	1.31 %	0.0932	0.82 %	1490.2	17.4	1492.9	15.4	1492.9	15.4
EJD-007_111	151	0.58	5.6904	1.42 %	0.0736	1.09 %	1043.6	13.6	1030.4	21.8	1030.4	21.8
EJD-007_112	214	0.38	3.8950	1.37 %	0.0926	0.95 %	1473.1	18.1	1479.6	18.0	1479.6	18.0
EJD-007_113	305	1.47	3.9407	1.36 %	0.0920	0.84 %	1457.9	17.7	1466.5	15.8	1466.5	15.8
EJD-007_114	113	1.46	5.8806	1.49 %	0.0715	1.24 %	1012.4	13.9	970.9	25.2	970.9	25.2
EJD-007_115	129	0.43	3.8176	1.38 %	0.0912	0.99 %	1499.8	18.4	1451.2	18.8	1451.2	18.8
EJD-007_116	124	0.63	5.9188	1.39 %	0.0714	1.33 %	1006.3	13.0	970.3	27.0	970.3	27.0
EJD-007_117	324	0.41	5.6983	1.43 %	0.0725	0.99 %	1042.3	13.8	999.3	20.0	999.3	20.0
EJD-007_118	43	0.39	5.2955	1.76 %	0.0769	1.57 %	1115.1	18.0	1119.1	31.0	1119.1	31.0
EJD-007 119	117	0.48	5.3849	1.48 %	0.0761	1.27 %	1098.1	15.0	1097.7	25.3	1097.7	25.3
EJ D-014_1	144	0.70	34.0290	1.65 %	0.0487	1.97 %	186.7	3.0	135.2	45.6	186.7	3.0
EJ D-014_2	76	0.83	34.5090	1.84 %	0.0479	2.97 %	184.1	3.3	94.0	69.0	184.1	3.3
EJ D-014_3	49	0.80	33.2921	1.87 %	0.0573	2.82 %	190.8	3.5	503.6	60.9	190.8	3.5
EJ D-014_4	115	0.84	35.0533	1.80 %	0.0484	2.72 %	181.3	3.2	117.6	63.0	181.3	3.2
EJ D-014_5	95	0.97	35.1982	1.89 %	0.0517	2.80 %	180.6	3.4	271.1	63.0	180.6	3.4
EJ D-014_6	245	1.46	33.5635	1.57 %	0.0511	1.69 %	189.3	2.9	244.7	38.5	189.3	2.9
EJ D-014_7	118	0.48	33.0719	1.73 %	0.0504	2.29 %	192.0	3.3	214.3	52.1	192.0	3.3
EJ D-014_8	86	0.78	34.1784	2.00 %	0.0487	2.42 %	185.9	3.7	131.0	56.0	185.9	3.7
EJ D-014_9	195	0.44	33.6192	1.53 %	0.0503	2.14 %	189.0	2.9	208.8	48.9	189.0	2.9
EJ D-014_10	108	0.77	34.8259	1.78 %	0.0485	2.58 %	182.5	3.2	122.3	59.6	182.5	3.2
EJD-014_11	86	1.13	31.9410	2.12 %	0.0505	3.31 %	198.7	4.1	217.1	75.0	198.7	4.1
EJ D-014_12	68	0.70	33.8455	1.88 %	0.0506	3.49 %	187.7	3.5	224.0	78.7	187.7	3.5
EJ D-014_13	94	1.06	34.3856	2.20 %	0.0516	3.28 %	184.8	4.0	267.8	73.6	184.8	4.0
EJ D-014_14	59	0.75	36.4773	1.71 %	0.0530	3.08 %	174.3	2.9	329.6	68.5	174.3	2.9
EJ D-014_15	143	0.84	33.5728	1.99 %	0.0504	2.18 %	189.2	3.7	212.8	49.7	189.2	3.7

Sample	U	Th	238U	1 sigma	207Pb	1 sigma	206/238 (^{207}corr)	1 sigma	207/206	1 sigma	Best age	1 sigma
Name	ppm	U	206Pb	% error	206Pb	% error	age	abs err	age	abs err		abs err Ma
EJ D-014_16	73	0.86	34.6124	1.91 %	0.0497	3.34 %	183.6	3.5	178.6	76.0	183.6	3.5
EJ D-014_17	104	1.41	34.6468	2.11 %	0.0599	2.05 %	183.4	3.8	601.6	43.8	183.4	3.8
EJ D-014_18	67	1.05	34.0045	1.99 %	0.0528	3.44 %	186.8	3.7	319.4	76.3	186.8	3.7
EJ D-014_19	134	0.93	34.3436	1.58 %	0.0510	2.01 %	185.0	2.9	239.9	45.8	185.0	2.9
EJ D-014_20	80	0.74	33.4360	1.82 %	0.0539	2.63 %	190.0	3.4	368.8	58.1	190.0	3.4
EJ D-014_21	462	1.27	33.4358	1.60 %	0.0512	1.68 %	190.0	3.0	250.3	38.2	190.0	3.0
EJ D-014_22	75	0.98	33.3752	2.21 %	0.0503	3.11 %	190.3	4.1	208.1	70.6	190.3	4.1
EJ D-014_23	96	0.87	34.4966	1.70 %	0.0531	2.59 %	184.2	3.1	334.2	57.7	184.2	3.1
EJ D-014_24	202	0.91	33.7127	1.85 %	0.0492	2.19 %	188.4	3.4	156.7	50.4	188.4	3.4
EJ D-014_25	81	1.54	34.4314	1.92 %	0.0530	2.65 %	184.6	3.5	328.9	59.0	184.6	3.5
EJ D-014_26	545	0.76	33.1057	1.57 %	0.0489	1.25 %	191.8	3.0	142.2	29.1	191.8	3.0
EJ D-014_27	52	1.00	35.7610	1.85 %	0.0503	3.19 %	177.8	3.2	207.5	72.2	177.8	3.2
EJ D-014_28	64	1.20	6.3829	1.56 %	0.0713	1.36 %	938.2	13.6	967.0	27.5	967.0	27.5
EJ D-014_29	96	0.69	35.8225	2.03 %	0.0531	3.03 %	177.5	3.5	335.0	67.2	177.5	3.5
EJ D-014_30	110	0.82	36.5592	2.34 %	0.0662	2.42 %	174.0	4.0	813.8	49.7	174.0	4.0
EJ D-014_31	147	0.96	37.5797	1.52 %	0.0472	1.60 %	169.3	2.5	58.2	37.7	169.3	2.5
EJ D-014_32	65	1.01	36.7213	1.96 %	0.0489	3.63 %	173.2	3.4	144.4	83.1	173.2	3.4
EJ D-014_33	80	0.92	37.4399	1.64 %	0.0491	3.13 %	169.9	2.8	153.8	71.6	169.9	2.8
EJ D-014_34	209	0.51	36.4610	1.28 %	0.0508	1.56 %	174.4	2.2	230.5	35.6	174.4	2.2
EJ D-014_35	115	0.76	36.6783	1.59 %	0.0519	2.23 %	173.4	2.7	279.4	50.2	173.4	2.7
EJ D-014_36	79	0.78	37.3049	1.76 %	0.0479	3.36 %	170.5	3.0	93.7	77.7	170.5	3.0
EJ D-014_37	150	0.81	6.5081	1.78 %	0.0725	0.78 %	921.4	15.3	1000.6	15.8	1000.6	15.8
EJ D-014_38	190	1.03	37.0763	1.38 %	0.0483	1.63 %	171.6	2.3	112.7	38.0	171.6	2.3
EJ D-014_39	364	1.21	38.5246	2.89 %	0.0490	3.75 %	165.2	4.7	150.1	85.7	165.2	4.7
EJ D-014_40	100	0.72	37.6531	1.70 %	0.0506	2.99 %	169.0	2.8	222.3	67.7	169.0	2.8
EJ D-014_41	105	1.09	36.8380	1.51 %	0.0512	2.86 %	172.7	2.6	248.0	64.5	172.7	2.6
EJ D-014_42	144	1.01	37.4558	1.82 %	0.0541	2.48 %	169.8	3.1	376.8	54.9	169.8	3.1
EJ D-014_43	184	1.24	35.9910	1.80 %	0.0487	1.70 %	176.7	3.1	134.2	39.4	176.7	3.1
EJ D-014_44	84	0.84	37.4435	3.39 %	0.0750	3.17 %	169.9	5.7	1068.2	62.5	169.9	5.7
EJ D-014_45	86	0.68	38.9281	2.07 %	0.0547	2.70 %	163.5	3.3	398.9	59.3	163.5	3.3
EJ D-014_46	149	1.29	33.9579	3.24 %	0.0667	2.28 %	187.1	6.0	828.2	46.9	187.1	6.0
EJ D-014_47	91	1.09	29.4568	3.17 %	0.0881	3.19 %	215.2	6.7	1384.9	60.1	215.2	6.7
EJ D-014_48	163	0.97	39.6320	2.34 %	0.0495	2.11 %	160.6	3.7	169.9	48.6	160.6	3.7
EJ D-014_49	133	0.80	36.9091	2.49 %	0.0507	2.22 %	172.3	4.2	225.8	50.5	172.3	4.2
EJ D-014_50	711	0.73	51.6484	2.44 %	0.0899	0.88 %	123.6	3.0	1424.0	16.8	123.6	3.0
EJ D-014_51	101	1.04	37.5235	2.05 %	0.0491	2.48 %	169.5	3.4	150.9	57.1	169.5	3.4
EJ D-014_52	165	1.02	37.3763	1.78 %	0.0522	2.23 %	170.2	3.0	293.1	50.1	170.2	3.0
EJ D-014_53	67	1.41	36.9132	2.05 %	0.0531	2.68 %	172.3	3.5	333.7	59.7	172.3	3.5
EJ D-014_54	63	0.71	37.2829	1.55 %	0.0462	3.55 %	170.6	2.6	8.1	83.3	170.6	2.6
EJ D-014_55	137	0.80	37.6257	1.46 %	0.0526	1.70 %	169.1	2.4	310.7	38.2	169.1	2.4
EJ D-014_56	156	0.91	35.7772	1.30 %	0.0481	2.34 %	177.7	2.3	105.8	54.5	177.7	2.3
EJ D-014_57	71	0.76	36.1509	4.90 %	0.1322	4.87 %	175.9	8.5	2128.0	82.8	2128.0	82.8
EJ D-014_58	136	0.89	36.6034	1.54 %	0.0521	2.15 %	173.8	2.6	288.2	48.3	173.8	2.6
EJ D-014_59	129	1.17	36.2361	3.04 %	0.0544	2.77 %	175.5	5.3	389.0	61.0	175.5	5.3
EJ D-014_60	92	0.96	37.2709	1.57 %	0.0502	3.11 %	170.7	2.7	203.4	70.7	170.7	2.7
EJ D-014_61	97	0.97	36.7139	1.75 %	0.0525	2.42 %	173.2	3.0	309.0	54.1	173.2	3.0
EJ D-014_62	94	1.06	37.5913	1.65 %	0.0496	2.20 %	169.2	2.8	176.5	50.5	169.2	2.8
EJ D-014_63	96	0.82	37.0241	1.54 %	0.0483	3.13 %	171.8	2.6	113.7	72.3	171.8	2.6
EJ D-014_64	532	0.72	42.4667	1.14 %	0.0515	1.11 %	150.0	1.7	261.5	25.3	150.0	1.7
EJ D-014_65	142	0.90	34.5198	1.44 %	0.0560	2.15 %	184.1	2.6	451.2	47.1	184.1	2.6
EJ D-014_66	149	0.38	34.6840	2.15 %	0.0512	2.22 %	183.2	3.9	250.8	50.3	183.2	3.9
EJ D-014_67	82	0.89	36.3195	1.80 %	0.0531	3.10 %	175.1	3.1	331.7	68.9	175.1	3.1
EJ D-014_68	103	0.99	36.6971	1.84 %	0.0515	2.43 %	173.3	3.2	264.7	54.7	173.3	3.2
EJ D-014_69	120	1.00	34.4158	1.62 %	0.0735	2.20 %	184.6	3.0	1028.1	43.9	184.6	3.0
EJ D-014_70	43	1.16	36.9330	2.26 %	0.0562	3.94 %	172.2	3.8	462.1	84.9	172.2	3.8
EJ D-014_71	211	0.61	35.0867	1.25 %	0.0527	1.88 %	181.2	2.2	316.8	42.1	181.2	2.2
EJ D-014_72	58	0.62	37.0287	1.77 %	0.0554	2.89 %	171.8	3.0	427.0	63.1	171.8	3.0
EJ D-014_73	127	1.08	38.2746	1.37 %	0.0485	2.37 %	166.3	2.2	122.4	54.9	166.3	2.2
EJ D-014_74	103	0.97	37.8862	1.53 %	0.0511	2.91 %	167.9	2.5	247.6	65.6	167.9	2.5
EJ D-014_75	169	1.13	38.1779	1.92 %	0.0547	1.98 %	166.7	3.2	398.7	43.7	166.7	3.2
EJ D-014_76	87	0.95	37.8314	2.28 %	0.0537	3.44 %	168.2	3.8	357.1	75.8	168.2	3.8
EJ D-014_77	172	0.58	36.0605	1.67 %	0.0490	1.72 %	176.3	2.9	150.1	39.8	176.3	2.9

Sample	U	Th	238U	1 sigma	207Pb	1 sigma	206/238 (^{207}corr)	1 sigma	207/206	1 sigma	Best age	1 sigma
Name	ppm	U	206Pb	% error	206Pb	% error	age	abs err	age	abs err		abs err Ma
EJ D-014_78	86	1.04	37.9678	1.81 %	0.0517	2.81 %	167.6	3.0	272.2	63.2	167.6	3.0
EJ D-014_79	129	0.80	37.1995	1.89 %	0.0493	2.59 %	171.0	3.2	160.4	59.6	171.0	3.2
EJ D-014_80	87	1.13	39.1557	2.05 %	0.0499	2.62 %	162.6	3.3	189.8	59.8	162.6	3.3
EJ D-014_81	130	1.50	34.4845	1.40 %	0.0595	2.23 %	184.3	2.6	585.9	47.6	184.3	2.6
EJ D-014_82	88	1.07	37.2493	1.93 %	0.0502	2.33 %	170.8	3.2	204.5	53.2	170.8	3.2
EJ D-014_83	177	1.28	37.3225	1.82 %	0.0489	2.14 %	170.4	3.1	144.9	49.5	170.4	3.1
EJ D-014_84	74	0.75	36.0157	1.75 %	0.0849	2.37 %	176.5	3.1	1313.7	45.3	176.5	3.1
EJ D-014_85	319	1.66	36.4016	1.55 %	0.0509	1.51 %	174.7	2.7	235.2	34.5	174.7	2.7
EJ D-014_86	163	1.04	36.9241	1.13 %	0.0480	2.03 %	172.3	1.9	101.4	47.3	172.3	1.9
EJ D-014_87	155	0.56	37.1450	1.63 %	0.0502	2.41 %	171.3	2.8	205.0	54.9	171.3	2.8
EJ D-014_88	42	0.74	39.1392	2.54 %	0.0679	2.96 %	162.6	4.1	864.8	60.3	162.6	4.1
EJ D-014_89	113	1.13	37.0998	1.36 %	0.0517	2.35 %	171.5	2.3	270.1	53.1	171.5	2.3
EJ D-014_90	73	0.68	36.2455	1.72 %	0.0536	3.10 %	175.4	3.0	356.0	68.6	175.4	3.0
EJ D-014_91	52	0.85	39.0135	2.00 %	0.0529	3.62 %	163.2	3.2	325.3	80.3	163.2	3.2
EJ D-014_92	373	0.84	36.3847	0.83 %	0.0494	1.30 %	174.8	1.4	168.2	30.1	174.8	1.4
EJ D-014_93	46	0.34	5.9802	1.05 %	0.0770	1.31 %	996.8	9.7	1121.4	25.9	1121.4	25.9
EJ D-014_94	228	0.64	37.8063	0.96 %	0.0487	1.89 %	168.3	1.6	135.2	43.8	168.3	1.6
EJ D-014_95	140	0.78	36.0444	1.35 %	0.0488	2.24 %	176.4	2.3	137.2	51.7	176.4	2.3
EJ D-014_96	91	0.91	35.5275	1.19 %	0.0497	2.95 %	178.9	2.1	181.8	67.4	178.9	2.1
EJ D-014_97	100	1.02	38.4890	1.50 %	0.0503	2.46 %	165.3	2.4	210.1	56.1	165.3	2.4
EJ D-014_98	128	0.84	36.2517	1.15 %	0.0496	2.53 %	175.4	2.0	178.1	57.9	175.4	2.0
EJ D-014_99	126	1.08	37.3389	1.06 %	0.0489	2.13 %	170.4	1.8	143.7	49.3	170.4	1.8
EJ D-014_100	89	1.07	37.1071	1.52 %	0.0523	3.09 %	171.4	2.6	299.5	69.1	171.4	2.6
EJ D-014_101	107	1.25	38.2261	1.29 %	0.0500	2.35 %	166.5	2.1	196.8	53.7	166.5	2.1
EJ D-014_102	76	0.99	37.7721	1.64 %	0.0495	2.93 %	168.4	2.7	171.5	67.0	168.4	2.7
EJ D-014_103	70	1.40	37.8836	1.81 %	0.0509	3.14 %	168.0	3.0	234.7	70.9	168.0	3.0
EJ D-014_104	26	0.65	36.1867	2.19 %	0.0596	4.88 %	175.7	3.8	587.9	102.4	175.7	3.8
EJ D-014_105	128	0.52	37.1316	0.98 %	0.0513	2.51 %	171.3	1.6	254.7	56.8	171.3	1.6
EJ D-014_106	55	0.65	36.6854	1.84 %	0.0521	3.40 %	173.4	3.1	289.6	75.8	173.4	3.1
EJ D-014_107	68	1.34	35.5551	1.69 %	0.0710	2.37 %	178.8	3.0	958.5	47.7	178.8	3.0
EJ D-014_108	53	1.02	37.3808	1.97 %	0.0499	3.49 %	170.2	3.3	191.1	79.2	170.2	3.3
EJ D-014_109	76	1.02	38.0831	1.43 %	0.0538	3.21 %	167.1	2.4	364.1	70.8	167.1	2.4
EJD-014_110	834	0.04	28.7195	0.70 %	0.0506	0.74 %	220.6	1.5	224.4	17.0	220.6	1.5
EJD-014_111	82	0.88	35.3760	4.21 %	0.0609	3.32 %	179.7	7.4	634.3	69.9	179.7	7.4
EJD-014_112	47	0.86	35.9277	2.39 %	0.0589	3.83 %	177.0	4.2	563.9	81.4	177.0	4.2
EJD-014_113	66	0.90	36.7502	1.82 %	0.0487	3.22 %	173.1	3.1	134.7	74.0	173.1	3.1
EJD-014_114	128	0.96	36.7727	1.34 %	0.0488	2.34 %	173.0	2.3	137.5	54.1	173.0	2.3
EJD-014_115	110	0.89	37.2498	1.25 %	0.0510	2.25 %	170.8	2.1	243.1	51.1	170.8	2.1
EJD-014_116	59	0.96	37.6749	1.65 %	0.0507	3.68 %	168.9	2.8	226.6	82.8	168.9	2.8
EJD-014_117	115	1.20	36.8628	1.44 %	0.0487	2.10 %	172.5	2.4	133.7	48.7	172.5	2.4
EJD-014_118	145	1.31	37.0817	1.11 %	0.0518	2.09 %	171.5	1.9	278.2	47.2	171.5	1.9
EJD-014_119	128	0.99	36.1308	1.33 %	0.0488	2.34 %	176.0	2.3	139.9	54.0	176.0	2.3
EJ D-014_120	110	1.26	35.6720	1.43 %	0.0523	2.43 %	178.2	2.5	297.8	54.6	178.2	2.5
EJ D-014_121	147	1.05	36.9320	1.31 %	0.0496	2.34 %	172.2	2.2	174.4	53.8	172.2	2.2
EJ D-014_122	200	0.99	38.3382	1.84 %	0.0530	1.90 %	166.0	3.0	327.1	42.6	166.0	3.0
EJ D-014_123	111	0.93	37.4997	1.44 %	0.0509	2.49 %	169.7	2.4	234.0	56.6	169.7	2.4
EJ D-014_124	175	1.42	38.7701	1.50 %	0.0498	2.00 %	164.2	2.4	186.9	45.9	164.2	2.4
EJ D-014_125	105	0.96	36.9894	1.55 %	0.0502	2.12 %	172.0	2.6	205.2	48.5	172.0	2.6
EJ D-014_126	109	0.98	37.2574	1.71 %	0.0514	2.51 %	170.7	2.9	257.6	56.6	170.7	2.9
EJ D-014_127	248	0.29	6.3002	1.31 %	0.0736	0.66 %	949.7	11.6	1030.1	13.3	1030.1	13.3
EJ D-014_128	54	0.61	38.1203	1.93 %	0.0520	3.90 %	166.9	3.2	286.7	86.9	166.9	3.2
EJ D-014_129	58	0.59	37.4508	2.23 %	0.0498	2.80 %	169.9	3.7	186.6	63.8	169.9	3.7
EJ D-014_130	1,122	0.92	23.9250	0.97 %	0.0520	0.79 %	264.0	2.5	286.0	17.9	264.0	2.5
EJ D-014_131	78	0.74	37.1104	1.61 %	0.0520	2.85 %	171.4	2.7	284.1	63.9	171.4	2.7
EJ D-014_132	192	0.46	37.2544	2.46 %	0.0555	3.16 %	170.8	4.1	430.9	68.8	170.8	4.1
EJD-014_133	147	1.25	36.3359	1.35 %	0.0514	1.85 %	175.0	2.3	260.6	42.0	175.0	2.3
EJ D-010_1	314	0.63	6.0036	1.64 %	0.0737	0.85 %	993.2	15.1	1033.9	17.1	1033.9	17.1
EJ D-010_2	151	0.64	4.6033	1.53 %	0.0827	1.01 %	1267.3	17.5	1262.0	19.5	1262.0	19.5
EJ D-010_3	292	1.16	36.0312	1.59 %	0.0509	1.83 %	176.5	2.8	235.2	41.7	176.5	2.8
EJ D-010_4	167	0.93	5.8086	1.51 %	0.0729	1.11 %	1024.0	14.3	1011.3	22.3	1011.3	22.3
EJ D-010_5	290	0.72	5.7704	1.41 %	0.0725	0.87 %	1030.3	13.4	999.4	17.5	999.4	17.5

Sample	U	Th	238U	1 sigma	207Pb	1 sigma	206/238 (^{207}corr)	1 sigma	207/206	1 sigma	Best age	1 sigma
Name	ppm	U	206Pb	% error	206Pb	% error	age	abs err	age	abs err		abs err Ma
EJ D-010_41	179	0.46	6.0340	1.73 %	0.0725	1.18 %	988.5	15.8	1001.4	23.8	1001.4	23.8
EJ D-010_42	309	1.06	6.2646	1.76 %	0.0770	1.01 %	954.7	15.6	1120.4	20.0	1120.4	20.0
EJ D-010_43	173	0.79	6.2086	2.18 %	0.0738	1.75 %	962.7	19.5	1034.7	34.9	1034.7	34.9
EJ D-010_44	1,183	0.41	6.7730	2.59 %	0.0831	0.76 %	887.8	21.5	1271.9	14.7	1271.9	14.7
EJ D-010_45	321	0.67	5.7232	1.56 %	0.0731	0.90 %	1038.1	14.9	1016.0	18.1	1016.0	18.1
EJ D-010_46	406	0.24	5.8600	1.51 %	0.0743	0.85 %	1015.7	14.2	1050.0	17.1	1050.0	17.1
EJ D-010_47	123	0.60	5.6822	1.61 %	0.0736	1.17 %	1045.0	15.5	1031.5	23.5	1031.5	23.5
EJ D-010_48	869	0.35	5.7497	1.45 %	0.0728	0.76 %	1033.7	13.8	1008.6	15.3	1008.6	15.3
EJ D-010_49	1,130	1.71	36.5239	1.54 %	0.0543	1.55 %	174.1	2.6	385.0	34.6	174.1	2.6
EJ D-010_50	284	0.24	5.3001	1.53 %	0.0767	0.90 %	1114.2	15.7	1113.7	17.8	1113.7	17.8
EJ D-010_51	953	1.09	5.9948	1.45 %	0.0728	0.72 %	994.5	13.3	1008.7	14.5	1008.7	14.5
EJ D-010_52	1,186	0.34	6.2968	1.61 %	0.0765	0.75 %	950.2	14.2	1108.3	15.0	1108.3	15.0
EJ D-010_53	417	1.71	37.1792	1.69 %	0.0498	1.86 %	171.1	2.8	183.5	42.8	171.1	2.8
EJ D-010_54	290	0.35	4.9997	1.59 %	0.0771	0.85 %	1175.4	17.1	1122.8	16.8	1122.8	16.8
EJ D-010_55	557	0.44	5.1219	1.49 %	0.0782	0.86 %	1149.7	15.6	1151.0	17.0	1151.0	17.0
EJ D-010_56	278	0.67	5.7291	1.59 %	0.0736	0.94 %	1037.1	15.2	1031.0	18.9	1031.0	18.9
EJ D-010_57	410	0.85	5.6951	1.57 %	0.0729	0.90 %	1042.8	15.1	1012.1	18.2	1012.1	18.2
EJ D-010_58	220	0.49	5.9143	1.76 %	0.0734	0.97 %	1007.0	16.4	1026.0	19.5	1026.0	19.5
EJ D-010_59	426	0.56	5.5730	1.49 %	0.0736	0.84 %	1063.9	14.6	1030.3	16.9	1030.3	16.9
EJ D-010_60	608	0.36	5.2426	1.45 %	0.0777	0.77 %	1125.4	15.0	1139.4	15.3	1139.4	15.3
EJ D-010_61	1,007	1.48	5.8434	1.46 %	0.0728	0.71 %	1018.3	13.7	1007.5	14.4	1007.5	14.4
EJ D-010_62	1,227	0.50	5.7720	1.43 %	0.0722	0.70 %	1030.0	13.6	992.8	14.2	992.8	14.2
EJ D-010_63	391	0.37	5.1989	1.50 %	0.0771	0.88 %	1134.1	15.6	1123.4	17.4	1123.4	17.4
EJ D-010_64	307	0.36	5.0949	1.53 %	0.0780	0.85 %	1155.3	16.1	1146.0	16.7	1146.0	16.7
EJ D-010_65	972	0.35	6.9689	1.63 %	0.0891	0.69 %	864.4	13.2	1407.1	13.2	1407.1	13.2
EJ D-010_66	708	0.38	5.7695	1.58 %	0.0727	0.74 %	1030.4	15.1	1006.1	14.9	1006.1	14.9
EJ D-010_67	484	0.59	5.9093	1.59 %	0.0753	0.94 %	1007.8	14.9	1077.1	18.7	1077.1	18.7
EJ D-010_68	252	1.34	36.6308	1.92 %	0.0493	2.31 %	173.6	3.3	161.7	53.1	173.6	3.3
EJ D-010_69	1,033	0.40	5.7473	1.59 %	0.0738	0.83 %	1034.1	15.2	1036.4	16.6	1036.4	16.6
EJ D-010_70	1,495	0.34	5.7710	1.58 %	0.0740	0.87 %	1030.2	15.1	1040.7	17.4	1040.7	17.4
EJ D-010_71	104	0.74	4.8387	1.84 %	0.0780	1.25 %	1211.0	20.3	1148.0	24.7	1148.0	24.7
EJ D-010_72	262	0.58	5.7796	1.48 %	0.0731	1.04 %	1028.7	14.1	1017.2	20.9	1017.2	20.9
EJ D-010_73	487	1.02	5.2190	2.44 %	0.0978	1.08 %	1130.1	25.3	1582.3	20.1	1582.3	20.1
EJ D-010_74	1,575	0.28	5.8781	1.62 %	0.0798	0.97 %	1012.8	15.1	1191.9	19.0	1191.9	19.0
EJ D-010_75	1,515	0.63	5.3548	1.48 %	0.0793	0.81 %	1103.7	15.0	1180.6	15.9	1180.6	15.9
EJ D-010_76	514	0.73	5.9587	1.54 %	0.0732	0.84 %	1000.1	14.3	1020.2	16.9	1020.2	16.9
EJ D-010_77	406	0.41	4.1873	1.47 %	0.0897	0.81 %	1380.5	18.3	1419.7	15.3	1419.7	15.3
EJ D-010_78	406	1.02	38.1133	1.81 %	0.0518	1.54 %	167.0	3.0	277.6	35.0	167.0	3.0
EJ D-010_79	212	1.43	37.8573	1.75 %	0.0486	2.37 %	168.1	2.9	129.4	54.8	168.1	2.9
EJ D-010_80	749	0.60	6.0126	1.53 %	0.0762	0.83 %	991.8	14.0	1100.0	16.5	1100.0	16.5
EJ D-010_81	1,131	0.43	3.7843	1.56 %	0.0951	0.76 %	1511.6	21.0	1529.2	14.2	1529.2	14.2
EJ D-010_82	513	0.55	5.5451	1.54 %	0.0782	0.74 %	1068.8	15.2	1152.8	14.6	1152.8	14.6
EJ D-010_83	964	1.22	5.8820	1.49 %	0.0733	0.79 %	1012.2	14.0	1023.1	15.8	1023.1	15.8
EJ D-010_84	655	0.64	6.0971	1.50 %	0.0736	0.84 %	979.0	13.6	1030.2	16.9	1030.2	16.9
EJ D-010_85	1,492	0.31	14.8976	1.95 %	0.0563	1.13 %	418.8	7.9	464.2	24.7	418.8	7.9
EJ D-010_86	195	0.74	5.2531	1.78 %	0.0771	1.06 %	1123.3	18.3	1125.0	21.0	1125.0	21.0
EJ D-010_87	559	0.71	6.0259	1.72 %	0.0729	0.88 %	989.8	15.8	1010.2	17.7	1010.2	17.7
EJ D-010_88	587	1.47	5.0517	1.57 %	0.0841	0.93 %	1164.3	16.7	1295.4	18.0	1295.4	18.0
EJ D-010_89	641	0.40	5.7638	1.48 %	0.0733	0.82 %	1031.4	14.1	1022.7	16.5	1022.7	16.5
EJ D-010_90	255	0.82	5.6116	1.43 %	0.0732	0.89 %	1057.2	14.0	1020.5	18.0	1020.5	18.0
EJ D-010_91	1,713	0.31	5.9394	1.84 %	0.0824	0.76 %	1003.1	17.1	1254.5	14.7	1254.5	14.7
EJ D-010_92	397	0.55	5.7799	1.57 %	0.0737	0.88 %	1028.7	14.9	1032.7	17.6	1032.7	17.6
EJ D-010_93	810	0.60	5.8511	1.49 %	0.0730	0.74 %	1017.1	14.0	1014.9	14.9	1014.9	14.9
EJ D-010_94	49	0.47	5.3694	1.82 %	0.0762	1.49 %	1101.0	18.4	1100.4	29.5	1100.4	29.5
EJ D-010_95	1,029	0.28	5.4165	1.43 %	0.0760	0.72 %	1092.2	14.3	1096.3	14.4	1096.3	14.4
EJ D-010_96	599	0.87	5.8895	1.43 %	0.0729	0.83 %	1011.0	13.4	1011.1	16.7	1011.1	16.7
EJ D-010_97	413	0.95	6.3364	1.54 %	0.0742	0.85 %	944.6	13.5	1046.1	17.1	1046.1	17.1
EJ D-010_98	1,981	0.45	5.0285	1.67 %	0.1009	0.79 %	1169.2	17.9	1641.4	14.6	1641.4	14.6
EJ D-010_99	857	0.40	5.9042	1.59 %	0.0729	0.85 %	1008.6	14.9	1011.9	17.1	1011.9	17.1
EJ D-010_100	185	0.34	5.3306	1.57 %	0.0764	0.96 %	1108.3	15.9	1105.5	19.0	1105.5	19.0
EJ D-010_101	839	0.53	5.8713	1.36 %	0.0802	0.81 %	1013.9	12.8	1202.9	15.8	1202.9	15.8
EJ D-010_102	61	0.70	5.7843	1.83 %	0.0733	1.50 %	1028.0	17.3	1022.7	30.0	1022.7	30.0

Sample	U	Th	238U	1 sigma	207Pb	1 sigma	206/238 (^{207}corr)	1 sigma	207/206	1 sigma	Best age	1 sigma
Name	ppm	U	206Pb	% error	206Pb	% error	age	abs err	age	abs err		abs err Ma
EJ D-010_103	254	0.57	5.7769	1.51 %	0.0743	0.92 %	1029.2	14.3	1048.6	18.4	1048.6	18.4
EJ D-010_104	1,112	0.38	5.2549	2.10 %	0.0772	0.83 %	1123.0	21.6	1125.6	16.5	1125.6	16.5
EJ D-010_106	100	0.94	5.8157	1.65 %	0.0786	1.38 %	1022.8	15.6	1161.7	27.1	1161.7	27.1
EJ D-010_107	1,326	0.23	5.7366	1.56 %	0.0745	0.69 %	1035.9	15.0	1055.5	13.9	1055.5	13.9
EJ D-010_108	113	0.40	5.1847	1.44 %	0.0771	1.05 %	1136.9	15.0	1123.3	20.8	1123.3	20.8
EJ D-010_109	721	0.52	5.7823	1.37 %	0.0737	0.76 %	1028.3	13.1	1033.6	15.4	1033.6	15.4
EJD-010_110	445	0.45	5.2336	1.56 %	0.0779	0.83 %	1127.2	16.1	1144.4	16.5	1144.4	16.5
EJD-010_111	676	0.79	5.7724	1.42 %	0.0740	0.81 %	1029.9	13.5	1040.3	16.3	1040.3	16.3
EJD-010_112	497	0.63	5.6984	1.44 %	0.0734	0.80 %	1042.3	13.9	1024.5	16.0	1024.5	16.0
EJD-010_113	318	0.65	5.9596	1.67 %	0.0735	0.99 %	1000.0	15.4	1026.4	19.8	1026.4	19.8
EJD-010_114	996	0.75	3.5000	1.41 %	0.1038	0.70 %	1620.1	20.2	1693.3	12.8	1693.3	12.8
EJD-010_115	519	0.50	5.3604	1.44 %	0.0796	0.83 %	1102.7	14.6	1186.2	16.2	1186.2	16.2
EJD-010_116	362	0.82	5.7353	1.48 %	0.0734	0.80 %	1036.1	14.2	1026.2	16.1	1026.2	16.1

A2.
CONCORDIA CHART

El Ocal Section | **El Cobre Section**

Upper Member

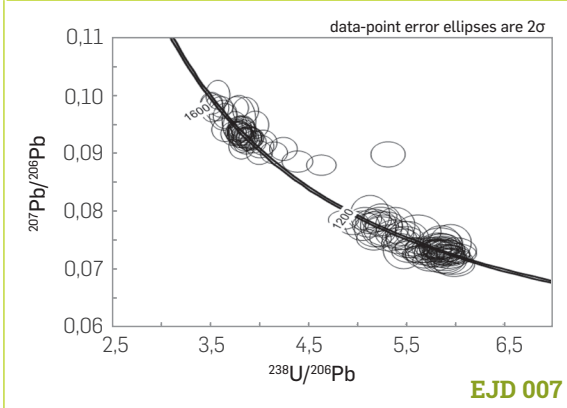

EJD 007

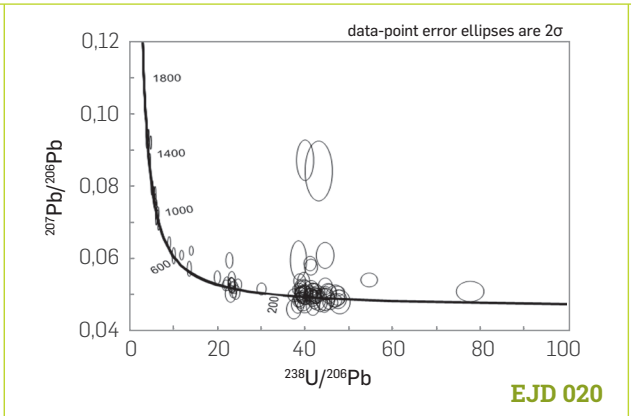

EJD 020

Lower Member

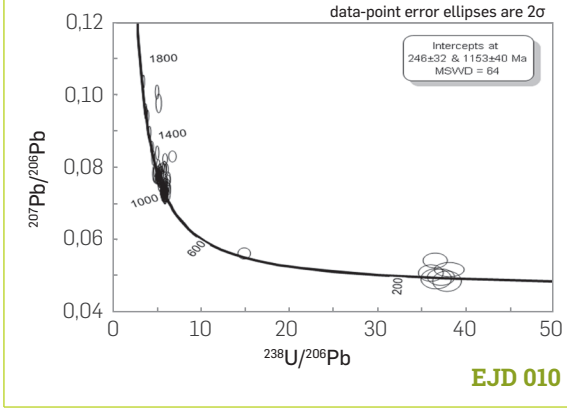

EJD 010

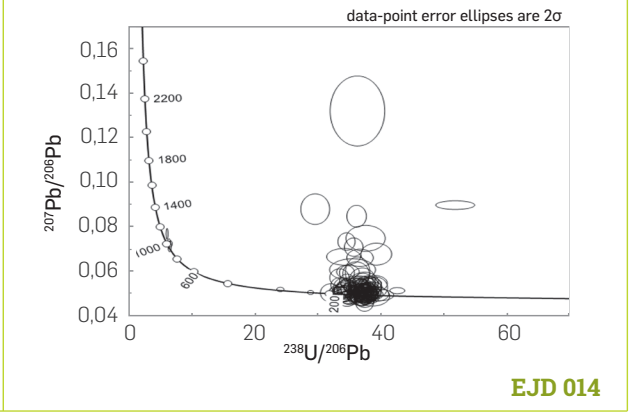

EJD 014